

Review

The Effect of Addition of Nanoparticles, Especially ZrO₂-Based, on Tribological Behavior of Lubricants

Adam Rylski ¹ and Krzysztof Siczek ^{2,*} 

¹ Institute of Materials Science and Engineering, Lodz University of Technology, 90-924 Lodz, Poland; adam.rylski@p.lodz.pl

² Department of Vehicles and Fundamentals of Machine Design, Lodz University of Technology, 90-537 Lodz, Poland

* Correspondence: ks670907@p.lodz.pl

Received: 28 December 2019; Accepted: 24 February 2020; Published: 2 March 2020



Abstract: The aim of the paper was to discuss different effects, such as, among others, agglomeration of selected nanoparticles, particularly those from zirconia, on the tribological behavior of lubricants. The explanation of the difference between the concepts of ‘aggregation’ and ‘agglomeration’ for ZrO₂ nanoparticles is included. The factors that influence such an agglomeration are considered. Classification and thickeners of grease, the role of additives therein, and characteristics of the lithium grease with and without ZrO₂ additive are discussed in the paper. The role of nanoparticles, including those from ZrO₂ utilized as additives to lubricants, particularly to the lithium grease, is also discussed. The methods of preparation of ZrO₂ nanoparticles are described in the paper. The agglomeration of ZrO₂ nanoparticles and methods to prevent it and the lubrication mechanism of the lithium nanogrease and its tribological evaluation are also discussed. Sample preparation and a ball-on disc tester for investigating of spinning friction are described. The effect of ZrO₂ nanoparticles agglomeration on the frictional properties of the lithium grease is shown. The addition of 1 wt.% ZrO₂ nanoparticles to pure lithium grease can decrease the friction coefficient to 50%. On the other hand, the agglomeration of ZrO₂ nanoparticles in the lithium grease can increase twice the friction coefficient relative to that for the pure grease.

Keywords: friction; lithium grease; addition of ZrO₂ nanoparticles; nanoparticle agglomeration

1. Introduction

Grease is a largely used semi-solid lubricant composed of base oil, thickeners and, optionally, of improvers. It is often used in roller bearing systems when the supply of the indispensable oil through the central lubrication system is difficult or even impossible, or when the lubricant must remain in a closed space [1]. The presence of grease supports the sealing process of bearings, as it is resistant to leakage, prevents to some extent the occurrence of corrosion of mating surfaces, and requires uncomplicated maintenance. The grease has a complex microstructure that is subjected to degradation during prolonged use. Grease is a thixotropic body, whose properties change over time under the influence of shear stresses [2], in a partially reversible manner [3]. Paszkowski [4] investigated lithium grease using a rotary rheometer. He found that both the thickener fraction and shear rate significantly affected reconstruction of the lithium thickener microstructure after friction.

Greases, especially the lithium ones, are largely used for lubrication of rolling bearings and mobile connections in automotive and other industries. Such friction associations can be highly loaded, however, under the condition that they operate under not very high values of slip speed and temperature.

1.1. Degradation Systems of Greases

During operation of rolling bearings mounted in various mechanical devices, the process of mechanical degradation of lithium grease is commonly observed in result of changes in the bulk properties of grease due to shear stresses acting on it during friction.

Two degradation mechanisms of greases are described in the literature: physical degradation and the chemical one [5–8]. Physical degradation includes mechanical degradation of the thickener structure as a result of shear stress, separation of base oil and thickener, evaporation of base oil, and grease contamination by pollutants and debris. Chemical degradation [9,10] includes oxidation of both base oil and thickener, as well as depletion of improvers. Chemical degradation dominates during bearing operation at a higher temperature. The mechanical degradation of grease is prevailing when the bearing system is operating at high speed [11]. Most often, both chemical and physical degradation occur due to the changing operating conditions of rolling bearings, which largely depend on the chemical composition of grease [12]. Very favorable conditions for degradation arise when different lubricants are mixed containing components that are prone to react with each other.

Rezasoltani and Khonsari [8] described other mechanisms of grease degradation, such as grease flow resulting in its starvation. However, this should be considered as a malfunction of the lubrication system rather than the mechanism of degradation of the grease itself. Shearing lithium complex greases in a rheometer at a temperature range 25–45 °C, they obtained a linear relationship between the generated entropy and the grease aging manifested by changes in consistency [13]. They built a shear life model [14] allowing determination of the grease life by means of time necessary to reach the critical consistency.

Hurley et al. [15] found that lithium hydroxystearate grease may be oxidized and thermally degraded. Couronne and Vergne [16] found that at elevated temperature (150 °C), lithium grease was weakened, even in the absence of oxygen. Plint and Alliston-Greiner [17] found that during aging of lithium grease at elevated temperature, the effect of shearing on loss of its viscosity was more pronounced. Cyriac et al. [18] reported a two-fold reduction of yield stress with a certain temperature increase for both lithium- and polyurea-thickened greases. A decrease in the yield stress of the lithium grease at elevated temperature was reported in Reference [19]. Ide et al. [20] found the activation energy based on Arrhenius's law as an appropriate parameter for life prediction of lithium greases.

According to Zhou et al. [21], the mechanical degradation of grease is caused by pressure and shear stresses. According to Reference [22], grease may soften during aging and leak out of the bearing systems. Grease may also stiffen, causing a loss of oil bleeding capacity [6,16,23]. Such an aging behavior of grease depends on the temperature, chemical composition of the grease, and its thickener microstructure. The elevated temperatures accelerate aging due to likely changes in thickener properties [23–25].

Zhou et al. [21] studied the mechanical aging behavior of fibrous structured greases, such as the lithium complex soap with poly-alpha-olefin (PAO) base oil and the polyurea-thickened grease with ester base oil. They reported that in the absence of oxygen no chemical reactions occurred. They found that the shear degradation of grease was accelerated with an increase in temperature, according to the Arrhenius law. They created a grease aging master curve describing the effect of shear and temperature on the mechanical aging of the grease under investigation.

According to Reference [11], if the operating temperature is significantly lower than the oxidation one and there is no contamination or evaporation of the grease, the life of grease is determined by mechanical degradation.

1.2. The Aggregation and Agglomeration of Nanoparticles Dispersed in Grease

A certain strategy is readily used in the design of new devices or in their modifications. It is based on the use of the same tribological associations but operating under conditions of increased thermal and/or mechanical loads.

This is mainly due to overwhelming necessity of cost reduction applied to proven structures and materials or practices related to their maintenance, such as selection of proper lubricants. This approach requires changing composition of grease used so far, adapting its viscosity and stability to given operating conditions. One of the possible solutions to the problem is to disperse some amount of metal or non-metal nanoparticles in the base grease. It turned out that a barrier for wide application of this solution was occurrence of agglomerations of the dispersed nanoparticles. The term 'agglomeration' is frequently interchangeably called 'aggregation' and has led to confusion based on the phenomenological ground [26].

Aggregation and agglomeration are two different concepts used to describe a given set of particles or nanoparticles in a material. Both concepts have different meanings. Clustering of particles by aggregation is a reversible process, while clustering of particles through agglomeration is an irreversible process [26]. Both processes are difficult to distinguish using conventional techniques such as dynamic light scattering (DLS) [27], nanoparticle tracking analysis (NTA) [28], or electron microscopy imaging (EMI) [24]. Such techniques reveal large aggregates of particles in the investigated material only in general. Aggregations and agglomerations of particles in a material sample were created due to different mechanisms. One of these mechanisms consists of collisions and gluing of particles as a result of their random Brownian motion (Brownian agglomerations). Another mechanism called 'gravitational agglomeration' depends strictly on the particles' size and their final velocities. Slowly settling particles are captured by faster settling ones, which results in the formation of clusters of particles. Particle clustering affects the degree of acidity pH and ionic bonding strength. Therefore, methods for proper determination of the degree of aggregation and agglomeration of nanoparticles in a material sample are very important.

Phenomena of formation leading to binary and doped metal oxide nanoparticles were described in several papers ([29,30] and [31,32], respectively). The mechanisms of secondary particle formation during the nonaqueous synthesis influenced subsequently dispersing [33], functionalization [34,35], or surface property tailoring [36,37].

Smoluchowski [38] first approached the colloid aggregation and agglomeration with a mathematical particle size-dependent model. That so-called Diffusion-Limited Colloid Agglomeration (DLCA) model described the interparticle collision rate driven by Brownian motion. According to Mersmann [39], particle agglomeration induced by Brownian motion is known as 'perikinetic' one, whereas agglomeration caused by hydrodynamic forces is called 'orthokinetic'.

Zhang et al. [40] described the Reaction-Limited Colloid (perikinetic) Agglomeration (RLCA) model, where agglomeration was limited by the binding reaction between particles. This limitation is described by the attachment efficiency (α) corresponding to the probability of interparticle adherence after collision. According to Reference [41], the abovementioned limitation can be described with the Fuchs stability ratio (W), referring to the colloidal stability (the inverse of the attachment efficiency $W = 1/\alpha$).

Hotze et al. [42] presented the Derjaguin–Landau–Verwey–Overbeek theory describing nanoparticle agglomeration in aqueous media. The theory allowed the formulation of the attachment efficiency and Fuchs ratio. Such factors representing the difference between DLCA and RLCA resulted from the colloid integration reaction or stabilizing mechanisms hindering interparticle adherence.

Stolzenburg et al. [43] studied the secondary particle formation processes during the nonaqueous synthesis of ZrO₂ and TiO₂ nanoparticles and described mechanisms driving aggregation and agglomeration (Figure 1). They found that densely packed aggregates composed of primary nanoparticles were formed at the beginning, and next agglomerated to so-called 'superstructures'.

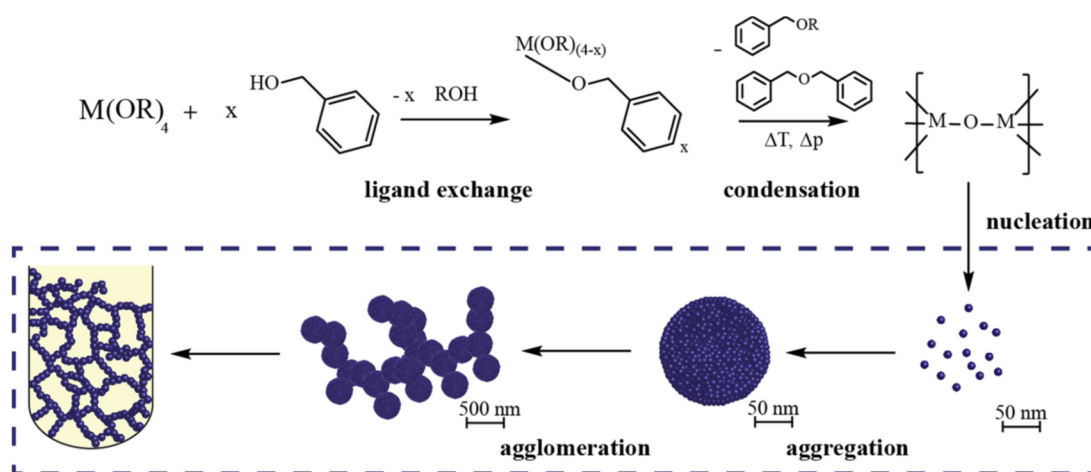


Figure 1. Particle formation mechanisms during the nonaqueous synthesis with an emphasis on the aggregation and agglomeration processes [43]. Reprinted with permission from (Stolzenburg, P.; Hämisch, B.; Richter, S.; Huber, K.; Garnweitner, G. Secondary Particle Formation during the Nonaqueous Synthesis of Metal Oxide Nanocrystals. *Langmuir* 2018, vol. 34(43) pp. 12834–12844, <https://doi.org/10.1021/acs.langmuir.8b00020>). Copyright (2018) American Chemical Society.

The development of particle size over the course of a standard ZrO_2 and TiO_2 nanoparticle synthesis is shown in Figure 2. The development shows an almost exponential trend.

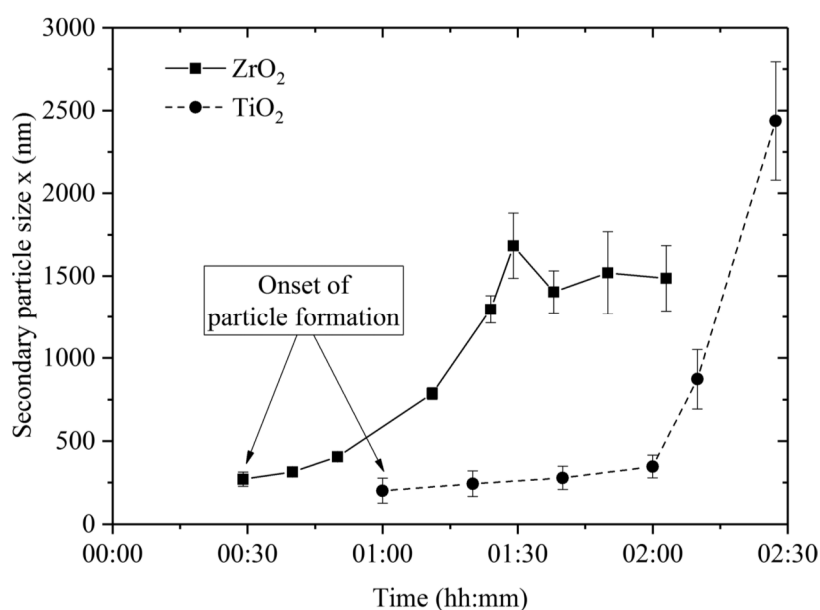


Figure 2. Agglomeration during a zirconia and titania synthesis under standard conditions [43]. Reprinted with permission from (Stolzenburg, P.; Hämisch, B.; Richter, S.; Huber, K.; Garnweitner, G. Secondary Particle Formation during the Nonaqueous Synthesis of Metal Oxide Nanocrystals. *Langmuir* 2018, vol. 34(43) pp. 12834–12844, <https://doi.org/10.1021/acs.langmuir.8b00020>). Copyright (2018) American Chemical Society.

Rizzuti et al. [44] studied a hydrothermal zirconia nanoparticle synthesis and observed spherical aggregate structures composed of 8 nm-sized particles. These structures further agglomerated to superstructures.

Rodríguez-Devecchis et al. [45] reported that the nanoparticles added to oil lubricant tended to agglomeration.

Jazaa et al. [46] found that once agglomeration occurs, the particle size changes. In order to better estimate the nominal particle size in the solution, the size distribution of the dispersed nanoparticles in PAO should be measured with the use of dynamic light scattering (DLS) technique. The theory underlying the measurements with this method is based on the effects of Brownian motion of nanoparticles on Rayleigh light scattering data. This allows determination of the size of a particle or molecule in the solution [47]. Jazaa et al. [46] explained that the primary result obtained from a DLS measurement represented the intensity-weighted mean diameter derived from the cumulations. Such a diameter was very sensitive to the existence of nanoparticle agglomeration due to the inherent intensity weighting.

1.3. Factors Affecting the Agglomeration

According to Reference [48], the agglomeration of the nanoparticles is important for lubricants as it affects the sedimentation rate and there is a loss of wear and ability to decrease the coefficient of friction (COF). In the case of poor dispersion stability, sedimentation and clogging may occur. The stable suspension in which particles do not form agglomerates at a significant rate allows an effective nanolubrication.

The agglomeration of nanoparticles can be undesirable not only during the preparation of nanolubricants but also during sintering. According to References [49,50], parameters of granulometry, such as shape and size of particles and their agglomerates or aggregates, both chemical and phase composition of initial powders, and the agglomerate or aggregate type affect compaction level and sintering process. The so-called 'soft' agglomerates are characterized by weak van der Waals forces between particles that can be easily separated in a liquid medium by ultrasonic treatment or/and addition of dispersants. The so-called 'hard' agglomerates are characterized by strong forces between particles due to high-temperature calcinations or inappropriate chemical additions.

According to References [51,52], the agglomeration kinetics of TiO₂ nanoparticles synthesized by aqueous sol-gel processes highly depended on pH level, temperature, and ionic bond strength.

Shih et al. [53] studied the stability of TiO₂ nanoparticle suspensions and found that the system destabilized and nanoparticles began to agglomerate at a certain salt concentration (at so-called 'critical coagulation concentration').

Padovini et al. [54] analyzed a hydrothermal zirconia nanoparticle synthesis and found that ZrO₂ nanoparticles directly formed amorphous microspheres before the primary particles crystallized within these structures.

Focusing on the effect of NH₄OH water solution concentration, the authors of Reference [55] studied the effect of coprecipitation conditions during the synthesis of ultrafine yttria-stabilized zirconia (YSZ) nanoparticles and gadolinium-doped YSZ. The use of 1 M or 5 M of NH₄OH led to a similar grain size of less than 6 nm. However, greater concentration led to a much greater fraction of agglomerated nanoparticles. This was due to an increased ionic bond force between particles caused by the high-temperature calcination or inappropriate chemical additions.

Some papers showed a clear relationship between tribological properties of the lubricant containing nanoparticles and their agglomerations.

During studies on graphite nanoparticles dispersed in palm oil [56] the COF value of nanolubricants increased after using the magnetic stirrer and the overhead stirrer. It was due to the agglomeration of nanoparticles that adversely affected the friction performance.

Moshkovith et al. [57] found that decreasing the agglomeration size increased the frequency of the nanoparticle penetrations into the contact area, thus reducing the COF value. The size of agglomerates of the nanoparticles decreases with the long-term mixing process.

Xie et al. [58] reported that poor dispersion stability increased the tendency of nanoparticles to agglomerate and, in turn, to a lesser friction performance.

According to References [56,59], the agglomeration of nanoparticles was conducive to a greater wear rate. The tribological performance of nanolubricants depended on the dispersion stability.

According to Reference [60], the ZrO₂ nanoparticles make an easier sintering process. The ordered agglomeration of zirconia primary crystallites into secondary particle assemblies ensures their homogeneous packing. However, size reduction of ZrO₂ nanoparticles also promotes undesirable disordered agglomeration. The assembled crystallites obtained during ordered and disordered agglomeration exposed to intense electromagnetic radiation can agglomerate even further.

The preliminary analysis of the nanopowder market, particularly in Poland, has shown that zirconia nanopowders are available on the market and are relatively cheap. The number of available publications on the use of ZrO₂ nanoparticles as an additive to lubricants is not great; nevertheless, the results of preliminary studies carried out by Wozniak et al. [61] pointed such nanoparticles as a candidate improving the tribological properties of some lubricants. It has been noted that the problem of agglomeration may also occur during preparation of nanolubricants with zirconia nanoparticles.

2. Components of Greases and Their Effect on Grease Properties

2.1. Classification and Thickeners of Greases

There are several classifications of greases. According to Reference [62], greases are classified according to their thickener composition, and on their consistency, according to the NLGI (National Lubricating Grease Institute) classification. This classification is characterized by 9 grades, depending on the so-called Worked Penetration Range. There are two major families of greases containing soap and non-soap thickeners. More than 90% of the thickeners used worldwide are soap-based.

There are three types of soap-based thickeners [62]:

- Simple soap—obtained from the reaction of one fatty acid, such as 12-hydroxystearic acid (12 HSA), and a metallic hydroxide, such as lithium hydroxide. The metallic hydroxide defines the thickener type. In the described case, the grease is called ‘simple lithium soap’.
- Mixed soap—obtained from the reaction of a fatty acid with two metallic hydroxides. For example, if the 12 HSA reacted with lithium and calcium hydroxide, it resulted in a mixed Ca/Li soap.
- Complex soap—obtained from the reaction of a fatty acid, such as 12 HSA, with a short chain complexing acid, such azelaic one, conducive to a complex soap. If lithium hydroxide was used, the result was a lithium complex grease. This thickener type has much better high-temperature properties than a simple soap one.

Complex lithium soaps and simple lithium soaps are the most widely used [63] (their share in the world market exceeds 60% [64]).

Soap Greases category contains: Calcium (stearate or hydroxystearate) Soap Grease, Aluminum Soap Grease, Lithium (stearate or hydroxystearate) Soap Grease, Calcium Complex Soap Grease, Aluminum Complex Soap Grease, and Lithium Complex Soap Grease [65].

Non-Soap Greases category contains: Urea and Polyurea Grease, Bentonite Grease, and Other Non-Soap Greases, like Na Terephthalamate Grease, Copper Phthalocyanine Grease, Teflon (PTFE) Grease, Mica Grease, and Silica Gel Grease [65].

2.2. Characteristics of Lithium Grease

A very important feature of the lithium grease is its load-carrying capacity. The lithium grease with the CaF₂ addition has the load-carrying capacity up to 48% greater than the base lithium one [66].

Zhao et al. [67] reported that addition of nano-calcium borate (NCB) to the lithium grease resulted in a greater load-carrying capacity as compared to the simple lithium one. The pure lithium grease did not provide effective lubrication under a load exceeding 300 N. Contrary to that, the grease with 6 wt.% of NCB exhibited good performance under the load up to 600 N.

It turned out as well during the study of the lithium grease with addition of CeF₃ nanoclusters surface capped with oleic acid (OA) that its load-bearing capacity was higher than that for the simple lithium one. The OA–CeF₃ nanocluster as the additive improved the resistance to wear and to extreme

pressure of the synthetic lithium grease. However, the OA-CeF₃ nanoclusters had only a little effect on the friction-reducing behavior of the lithium grease [68].

It was shown in another investigation of lithium grease with CaCO₃ nanoparticles [69] that the load-carrying capacity was greater than that of the simple lithium one. Moreover, Prakash et al. [70] reported that addition of CaCO₃ nanoparticles was conducive to lower wear and friction, greater load-carrying capacity, and resistance to extreme pressures in comparison to those of simple lithium grease.

Liu et al. [71] studied tribological behavior of amorphous overbased calcium sulfonate (AOBCS) and crystalline overbased calcium sulfonate (COBCS, transformed from the AOBCS) added to lithium complex grease. Addition of COBCS to the grease was conducive to lower friction and wear and greater load-carrying capacity in comparison to simple lithium grease. Addition of AOBCS particles improved tribological properties of complex lithium grease to a greater extent than the COBCS ones at similar concentration and load in contact zone.

It follows from the results mentioned above that rheology of the lithium grease is affected by use of nano-additives [72]. The rheological properties of the lithium grease were investigated in either static conditions or under steady-state (dynamic) conditions.

Addition of nano-calcium borate [67] to the lithium grease caused a slight decrease of the unworked penetration (measured according to ASTM D217 and D1403 standards).

Mohamed et al. [72] studied the rheological behavior of lithium grease with addition of carbon nanotubes. As a result, its shear stress and apparent viscosity were increased up to 67% and 82%, respectively.

2.3. Additives to Greases

According to Reference [73], lithium-complex greases are usually stable and resistant to water and high temperature. Appropriately selected additives can also improve such characteristics as extreme pressure, anti-wear, rust, and corrosion. These greases are also in agreement with the NLGI's GC-LB specification requirements (where GC—wheel bearing greases performance class chosen from existing GA, GB, and GC ones, and LB—chassis greases performance class chosen from existing LA and LB ones). The lithium-complex greases need a significant amount of antimony-zinc or other types of additives to have good resistance to extreme pressure and to wear properties. In addition, lithium-complex greases should be accomplished with rust-inhibiting additives. To improve impermeability, lithium-complex greases usually require tackifiers, which are prone to deplete quickly in the presence of water.

According to Reference [74], the conventional additives to greases are, among others, antioxidants, anti-wear agents, corrosion inhibitors, extreme pressure agents, friction modifiers, and metal deactivators.

The authors of the paper [75] found that additives enhanced performance of grease and protected the grease and lubricated surfaces when it was composed of mineral oil blended with a soap thickener.

According to Reference [76], greases cannot satisfy the requirements of high-performance lubricants without using the benefit of modern additives, such as corrosion inhibitors, as well as those increasing resistance to wear (so-called antiwear agents) and to extreme pressure (so-called extreme pressure agents).

The authors of the paper [77] reported on some rust inhibitors applied to the lithium grease:

- neutral calcium sulphonates characterized by high thermal stability and ability to inhibition of galvanic corrosion,
- medium base calcium sulphonates with Total Base Number (TBN) in a range (40–50), especially useful as all-purpose rust inhibitor for MoS₂ containing lithium greases. They can neutralize organic and inorganic acids.
- ethylenediamide sulphonate, the concentration of which in the lithium grease can reach 2 wt.%.

According to Reference [78], basic calcium sulfonate, neutral calcium sulfonate, and alkoxyated amine particles can be used as rust inhibitors in lithium greases.

According to Reference [79], the additives resistant to wear, also called antiwear (AW) ones, can be based on various P-, N-, and S-based chemical compounds. Dinonyldiphenylamines, octyl/butyldiphenylamines, 2,6 ditertbutylphenol derivatives, or methylene-bisdibutyldithiocarbamates can be utilized as the primary antioxidants in lithium and calcium greases. The Li-, Ca-, Ba-, Mg-, or Zn-based dinonylnaphthalenesulfonates can be utilized as the rust and oxidation inhibitors in such greases. Heterocyclic derivatives and also S- and N-based chemical compounds can be used as the yellow metal deactivators in the calcium and lithium greases. Amino acid derivatives with or without amines can be utilized as the rust inhibitors and they are synergistic with the phosphate esters, sulfurized olefins, triphenyl phosphorothionates (TPPT), and ashless dialkyldithiocarbamates used as the extremal pressure/antiwear (EP/AW) additives. The organic acid/ester compounds and zinc-based ones like zinc naphthenates can be used as rust inhibitors. Some of them can enhance the properties of EP/AW additives in the calcium and lithium greases. Furthermore, fatty acid esters, sulfurized fatty acid esters/triglycerides, and sulfurized α -olefins/triglycerides can be the EP/AW additives used in calcium and lithium greases.

Greases composed of mineral oil blended with soap thickener and additives have enhanced performance and protect well-lubricated surfaces [72].

Singh [80] showed that the blends of bis (1,5-diaryl-2,4-dithiomalonamido) dioxomolybdenum complexes with base lithium grease are greatly appreciated due to their resistance to extreme pressures. The greases reinforced with additives prevent rusting and corrosion of bearings and have better oxidation protection as compared to the greases without any additive.

Samy and Ali [81] studied contact of steel samples lubricated with lithium grease, contaminated with white cement grains and with addition of different tin content. The tests were carried out using a cross pin wear tester. The effect of the main components of white cement, such as lithium sand, kaolin, and limestone, on friction coefficient and wear of the tested samples was examined. It was found that tin as a solid lubricant dispersed in lithium grease reduces the abrasive wear of mating surfaces. Formation by the tin of a protective tribofilm on surfaces of steel samples and surfaces of particles of contaminants allowed to reduce the rate of the abrasive wear in the contact zone.

Friction coefficient was relatively greater when the lithium grease was contaminated with sand particles compared to that observed for the one contaminated with kaolin and limestone particles. The addition of sand particles was conducive to the greatest wear rates. The beneficial effect of tin was more pronounced at 5 wt.% content of sand particles. Addition of tin reduced the COF value and promoted the sliding of sand particles instead of abrasion. The decrease of the abrasive wear after addition of tin was more pronounced with increasing tin content up to 3 wt.%.

2.4. Nanoparticles as Additives to the Lubricant

2.4.1. The role of Nanoparticles as Additive to the Oil Lubricant

According to Reference [82], lubricating oil containing nanoparticles allows:

- micro-ball bearing-like operation between the mating surfaces;
- generation of protective film averting friction and smoothing the rough surface;
- repairing lubricated surface through fulfilling the wear tracks or apertures caused by loss of mass;
- polishing of mating surfaces via nanoparticles-assisted abrasion.

Hernández et al. [83] studied the resistance to wear of nanoparticles' suspensions in a polyalphaolefin (PAO 6) using a block-on-ring tribotester. ZrO₂ nanoparticles were separately dispersed at 0.5, 1.0, and 2.0 wt.% in PAO 6 using an ultrasonic bath for 2 min. As a result, friction and wear were reduced for all nanoparticle suspensions compared to the corresponding values registered for the base oil. The best result was obtained at 0.5 wt.% of ZrO₂. Neither agglomerations nor uniform depositions of ZrO₂ nanoparticles were found on the worn surfaces.

Battez et al. [84] studied the resistance to extreme pressure of CuO, ZnO, and ZrO₂ nanoparticles suspended in a polyalphaolefin (PAO 6) at amounts of 0.5, 1.0, and 2.0 wt.%. The dispersion of nanoparticles was obtained through an ultrasonic bath for 2 min. The resistance to extreme pressure (EP) was investigated with a four-ball (steel) EP lubricant tester. For all different contents of nanoparticles in PAO 6, the EP properties were better relative to the simple PAO 6. The resistance to EP was the best for CuO nanoparticles and the worst for ZrO₂ ones. The resistance to EP of ZrO₂ nanoparticles was same regardless of their content in PAO 6.

The authors of the paper [85] modified the surface of ZrO₂ nanoparticles with silane coupling agent KH-560 and dispersed them in 20# machine oil. They studied the tribological properties of such nano-lubricant with a four-ball tribotester and with a thrust-ring one. Addition of ZrO₂ nanoparticles to 20# machine oil was conducive to lack of wear and to COF value reduced up to 27% in comparison to the simple oil. The best result was obtained for the 0.5 wt.% of ZrO₂ nanoparticles.

Casado et al. [86] elaborated a procedure to chemically cap the surface of ZrO₂ nanoparticles (ZrO₂NPs) with long hydrocarbon chains (saturated C-8, C-10, and C-16) in order to obtain stable dispersions of ZrO₂NPs in lubricating oils without reducing their attributes as lubricant additives. During tribological tests with such nanolubricants, they found that dispersions of the long-chain capped ZrO₂NPs in base oils were conducive to low COF and wear rate values of base oils in comparison to those for raw lubricating oils.

Kumar et al. [87] studied tribological behavior of TiO₂ nanoparticles suspended in servo system lubricating oil through the sonication without adding any surfactant. They found that with an increase of volume concentrations (VC) of the nanoparticles, calorific value and flashpoint of the nano-lubricant decreased, whereas its viscosity remained unchanged. The wear rate and COF values increased due to agglomeration of TiO₂ nanoparticles caused by the lack of any surfactant during the preparation of the nano-lubricant.

Using the ball-on-disc tribotester, Yu et al. [88] studied the tribological properties of the Castor oil with different concentrations of MoS₂ nanoparticles. Addition of MoS₂ nanoparticles to the oil was conducive to low COF and adhesive wear rate values. However, MoS₂ nanoparticles in excessive concentration could agglomerate into large particles reducing the beneficial effects mentioned above.

Jendrzew et al. [89] dispersed in engine oil gold nanoparticles synthesized by pulsed laser ablation. After nine months, almost no agglomeration occurred. It was due to the attachment of engine oil additives or pyrolyzed/oxidized molecules to the nanoparticles limiting attractive interactions between nanoparticles.

Using a disc-on-disc tribotester, Hwang et al. [90] studied tribological properties of mineral oil with dispersed graphite and carbon black nanoparticles, graphite nanofibers, and carbon nanotubes. The nano-sized spherical particles suspended in mineral oil prevented direct contact between mating surfaces and significantly reduced the friction coefficient. Contrary to that, the fibrous nanoparticles with high aspect ratios deteriorated the lubrication between mating surfaces due to a higher degree of agglomeration.

Joly-Pottuz et al. [91] studied the effect of IF-WS₂ nanoparticles (IF-WS₂NPs, where IF means Inorganic Fullerene) concentration in PAO base oil at room temperature under the boundary lubrication regime. They found that the increase in the nanoparticles' concentration was conducive to low COF value compared to that for simple PAO oil even at very low concentration of IF-WS₂NPs as 0.1 wt.%. Above 1 wt.% of the NPs the COF value decreases. The same behavior was observed for IF-MoS₂ nanoparticles dispersed in base oil [92].

The authors of Reference [93] studied the effect of temperature on tribological performance of PAO blended with 1 wt.% of IF-MoS₂ nanoparticles at 20 °C and at 70 °C. They found a high and unstable COF value at 70 °C, whereas it was lower and more stable at 20 °C. It was due to an increased tendency of particles to agglomeration at a higher temperature.

Hu et al. [94] investigated the tribological behavior of hollow MoS₂ nanoparticles dispersed in liquid paraffin. At 1.5 wt.% of the nanoparticles, the COF and wear rate value were the lowest.

At higher concentrations, the probability for interparticle collisions was greater, which was conducive to an increased agglomeration of NPs.

Results of other tribological tests [95,96] showed that the Re-doped IF-MoS₂ nanoparticles were conducive to reduced agglomeration and produced stable suspensions in PAO base oil. Addition of undoped IF and 2H NPs was conducive to decrease of the COF value compared to that for the simple PAO oil. The Re-doped IF-MoS₂ NPs showed a two-fold lower value. It was due to improved dispersion of the Re-doped NPs and to increased conductivity of the tribofilm formed by those NPs, which inhibited tribocharging at the surface.

Aralihalli et al. [97] studied the tribological behavior of MoS₂ nanoparticles added to base oil with different surfactants, such as Aminopropyl trimethoxy silane (ATS), Sorbital monooleate (SPAN 80), Octadecyltrimethoxysilane (OTS), Perfluorodecyltriethoxysilane (PTS), and Perfluorooctyltrichlorosilane (PTCS). The lowest COF values were obtained for the mixtures containing ATS and SPAN. The particle size of MoS₂ NPs was smaller for these additives in comparison to the others. The molecules of the ATS and SPAN remained strongly grafted to the particles preventing agglomeration even under shear stresses, in contrast to other additives. The amine group bound covalently the molecules of ATS to MoS₂ while the hydrogen of the –OH groups combined with S atoms of MoS₂.

2.4.2. The Role of Nanoparticles as Additives in the Grease

Various aspects of nanoparticles used as additives and creating the so-called nanogrease were discussed in the review [98]. Nanogreases improve tribological properties, increase bearing capacity, and reduce wear, as compared to base oil grease. The enhanced performance of the nanogreases is due (among others) to their increased surface area to volume ratio.

Zhornik et al. [99] described the mechanism underlying the structure formation of the dispersed phase of greases when using the chemical principle of modification of complex calcium sulfonate grease by addition of nanocalcite particles.

Mohamed et al. [100] prepared calcium grease with different ratios of TiO₂ particles to carbon nanotubes TiO₂/CNTs (0.5, 1, 2, 3, 4 wt.%). They studied the tribological and rheological characteristics of nanogreases at different temperatures. Addition of TiO₂/CNTs at an optimal ratio of 3 wt.% was conducive to lower wear rate and COF values by 73% and 60%, respectively, compared to those for simple grease. The apparent viscosity and shear stress were increased by 48% and 74%, respectively.

Using a pin-on-disc tribotester, Mobasher et al. [101] studied tribological behavior of calcium grease with different concentration of multiwalled carbon nanotubes (MWCNTs) and Talc powder (at 1, 2, 3, 3 and 5 wt.%). The ratio of MWCNTs to Talc powder nanoparticles was equal to 1:1. Addition of 4 wt.% of MWCNTs/Talc NPs to calcium was conducive to lower wear rate and COF values by 81% and 64%, respectively, in comparison to simple grease. The obtained boundary film composed of MWCNTs, Talc powder nanoparticles, and other inorganic nanoparticle compounds was formed on the worn surface during friction tests. The thermal conductivity of nanogrease increased by 52%.

Younes et al. [102] obtained a stable and homogeneous nanogrease with PAO as base oil and carbon nanotubes as sole thickener. They found that carbon nanofiber (CNF), graphene, fullerene (C60), and Ni-coated single-wall carbon nanotube (SWNT) could not form stable greases as nanotubes did. The CNF/SWNT mixture did not form a stable grease, while Ni-coated SWNT/SWNT mixture did, due to the effect of intermolecular van der Waals forces. They stated that appropriate tube size (of nanotube and nanofiber), stereo structure (nanotube, graphene, and fullerene), and surface energy (nanotube and Ni-coated nanotube) were critical factors determining if van der Waals forces could have an effect or not.

Hu et al. [103] carried out comparative studies on tribological behavior among micro-MoS₂ (m-MoS₂), platelet-like nano-MoS₂, and spherical nano-MoS₂ particles added to lithium grease, lithium-calcium one and polyurea one, respectively. The m-MoS₂ slightly improved the lubrication properties of all studied greases. The nano-MoS₂ samples gave better results relative to the micro-MoS₂

particles. Tribofilms produced by nano-MoS₂ contained MoS₂ and MoO₃. Tribofilms produced by m-MoS₂ contained no Mo or only the MoO₃ form. The lack of MoS₂ form in tribofilms was conducive to poor lubrication of m-MoS₂ greases. The improved lubrication of the spherical nano-MoS₂ greases as compared with platelet-like nano-MoS₂ ones resulted from the lubricating superiority of the spherical structure in comparison to the platelet-like one.

2.4.3. Nanoparticles as Additive to Lithium Grease

Recently, some studies on the effect of different nanoparticles addition to the lithium grease on its tribological behavior were reported. SiO₂, ZrO₂, and TiO₂ nanoparticles were used.

He et al. [104] tested the lithium grease without and with an amount of SiO₂ nanoparticles using a four-ball tribotester. For the grease with 0.3 wt.% of SiO₂ nanoparticles, the friction coefficient was lowered by 26%–39% as compared to the case of the base grease, depending on loads in the contact zone.

Zhao et al. [67] prepared NCB addition with an average particle size of about 70 nm. They studied the friction and wear behavior of the NCB as additive to lithium grease using oscillating friction and wear tester. They found that the addition of NCB to the grease significantly improved its resistance to wear and the load-carrying capacity and, simultaneously, decreased its friction coefficient. The good tribological performance of NCB is affected by formation of a boundary film composed of deposited NCB and different products of tribochemical reactions, such as B₂O₃, CaO, and iron oxides on the rubbing surface.

The authors of the paper [105] studied the effect of addition of CNTs on tribological properties of the lithium grease. The CNTs of 10 nm average diameter and 5 μm in length were synthesized by electric arc discharge.

Xia et al. [106] studied changes of tribological properties of the lithium grease containing ZrO₂ nanoparticles as an additive. The friction coefficient decreased by over 30% after addition of 0.25% and 0.5% mass fractions of the ZrO₂ nanoparticles and the width of the wear scar decreased by 49% and 46%, respectively.

The authors of the paper [107] used eco-friendly carbon spheres (CS) of the size from 600 nm to 1 μm as an additive to lithium grease. The spheres were synthesized by hydrothermal synthesis. The obtained composite greases were evaluated with the use of HSR-2M ball-on-disk tester to explore the friction and wear at different mass fractions of the additive. When the content of the CS in the grease was 1 wt.% and the load 60 N, the friction coefficient decreased by more than 20% compared with that for the base grease. When the content of the CS additive was 1 wt.%, the worn surface was quite smooth with few tiny furrows and the wear volume decreased by more than 40% in comparison with that for the base grease. The lubricating mechanisms at CS additive consisted of ‘micro-roller’ effects, repairing, and forming the protective film.

Ashour et al. [108] using the Falex four-ball tester studied the effect of hybridized nanocomposite additive composed of multiwalled carbon nanotubes and multilayer nanographene platelets (MWCNTs)/(MLNGPs) onto tribological characteristics of lithium based-grease. The optimum concentration of MLNGPs was equal to 1 wt.%. Wear scar diameter (WSD) was reduced by 66%, friction coefficient was reduced by 91%, while maximum non-seizer load was increased by 90 kg over that for ordinary lithium grease. Studies of hybrid MWCNTs/MLNGPs additive showed that the optimum ratio of MLNGPs to MWCNTs was equal to 4:1.

Wang et al. [109] using the SRV-IV tribotester investigated tribological properties of lithium grease with additive from graphene–copper nanoparticles (GN/Cu NPs) composites. Such a composite was prepared by in situ chemical reduction in liquid phase. Grease samples with additives were prepared according to the procedure described in Reference [110]. The GN/Cu NPs composites allowed reduction of the wear loss of the disk by 85% and of the average COF value by 15% compared to the corresponding values for the base grease.

Ji et al. [69] obtained 45 nm-sized CaCO_3 nanoparticles through the carbonation process. They studied tribological properties of lithium grease containing the CaCO_3 nanoparticles using a four-ball tribotester. The CaCO_3 nanoparticles were conducive to lower wear and friction, good load-carrying capacity, and resisted to extreme pressures. During friction process, the worn surfaces were covered by the boundary films containing CaCO_3 , CaO, iron oxide, and other inorganic compounds.

Wang et al. [68] prepared CeF_3 nanocluster surface-capped with oleic acid (coded as OA- CeF_3) using extraction method. The effect of the OA- CeF_3 nanocluster as an additive to synthetic lithium grease was studied using a four-ball friction and wear tester. The as-prepared OA- CeF_3 nanocluster had a broad size distribution, with an average diameter value of approximately 20 nm. The oleic acid as the capping agent was chemically bonded to the CeF_3 nanocores via strong chemical bonds.

Zheng et al. [111] studied the friction and wear properties of lithium grease with addition of copper oxide (CuO) nanoparticles using a four-ball friction tester. The oil films were formed on wear surface providing decrease of friction and wear. When the content of CuO nanoparticles was 0.6 wt.%, only a small number of furrows were created on the wear surface. The lithium grease with CuO nanoparticles showed the lowest average friction coefficient and wear scar diameter, which were 30% and 13%, respectively, lower than those for pure lithium grease. CuO -containing oil films were detected on the wear surface. Appearance of the film lowered number of furrows and the roughness of wear surface, demonstrating the great role of CuO nanoparticles for improving tribological properties of the lithium grease.

A lithium grease with interesting additive of WS_2 nanoparticles of the size 50–200 nm was elaborated. The NanoLub[®] GH-X Lithium EP Grease Additive [112] is a surface-reconditioning nano-additive based on tungsten disulfide (WS_2) multilayered nano-fullerene particles. The grease containing such an additive has an exclusive resistance to Extreme Pressure (EP) and to wear and is characterized by low value of friction coefficient.

According to Reference [113], four complexes of rare earth hexadecylates (La, Pr, Sm, Gd) and copper hexadecylate were synthesized. Their tribological properties as additives to lithium grease were evaluated using a four-ball machine and a ring-block tester. These rare earth hexadecylates possessed antiwear and friction reduction properties in lithium grease. Their antiwear and friction reduction properties in lithium grease were better than that of copper hexadecylate. The tribochemical reaction happened during rubbing. The products of the tribochemical reaction improved the friction and wear behaviors of the lithium grease.

The authors of the paper [114] synthesized nanocrystallites of calcium fluoride (CaF_2) of the size of 60 nm by precipitation. The tribological properties of lithium grease with additive of such CaF_2 nanocrystallites were studied with a four-ball tribotester. The additive with such nanocrystallites exhibits excellent resistance to wear and to extreme pressure (EP) as well as a low value of friction coefficient. The EP and antiwear properties of the grease are non-proportionally affected by the content of CaF_2 nanocrystals. During tribological tests, the mating surfaces were covered by up to 12 nm thick boundary film. It was composed mainly of CaF_2 , CaO, iron oxide, and some organic compounds. Moreover, tribochemical reactions of CaF_2 nanocrystallites occurred on the worn steel surfaces at severe tribological conditions.

According to Reference [115], in order to improve the wear resistance of the mating surfaces, they were coated by strengthened brush plating through deposition of Bi nanoparticles. The latter were obtained via DC arc plasma evaporation. The tribological properties of lithium greases containing Bi nanoparticles were studied with a four-ball tribotester. The lithium grease containing as-prepared Bi nanoparticles showed significantly improved tribological properties and an increased load-carrying capacity in comparison with corresponding values for the base lithium grease.

According to Reference [116], tribological properties of lithium grease with different amounts of the layered compound of $\text{ZnS}(\text{NH}_2\text{CH}_2\text{CH}_2\text{NH}_2)_{0.5}$ was studied with a four-ball tribotester. Such grease showed good load-bearing capacity and resistance to wear. $\text{ZnS}(\text{NH}_2\text{CH}_2\text{CH}_2\text{NH}_2)_{0.5}$ additive to lithium grease showed better wear resistance than that for simple ZnS additive under similar test

conditions. It was due to that the two-dimensional structure of $\text{ZnS}(\text{NH}_2\text{CH}_2\text{CH}_2\text{NH}_2)_{0.5}$ with larger interface distances made the sliding process easier, and thus it improved the resistance to wear. The arisen tribofilm contained mainly FeS , ZnS , ZnO , Fe_xO_y , $\text{Fe}_u(\text{SO}_4)_v$, and ZnSO_4 compounds.

Using a ball-on-disc sliding wear tester, Chang et al. [117] studied the friction in the contact zone between a ball and a flat surface lubricated with TiO_2/CuO nanogrease. The tested lithium grease was synthesized with 0.5, 1.0, 1.5, and 2.0 wt.% of TiO_2/CuO nanoparticles dispersed therein. The TiO_2/CuO nanoparticle additives improved wear resistance of the lithium grease and decreased the COF value. It turned out that the greatest reduction of the friction and wear and significant reduction of the COF value by approximately 40% was obtained at 1.0 wt.% of TiO_2 nanoparticles in the grease. The wear of the lithium grease with a 2.0 wt.% content of CuO nanoparticles was lower by about 60% in comparison with that for pure lithium grease.

Rapoport et al. [118] obtained lithium grease (H3-Delkol) by mixing a mineral oil (30 cSt at 40 °C) with the lithium thickener. Such a base grease with 5 wt.% of layered 2H- MoS_2 particles (HM3-Delkol) was used as the reference one. In order to prepare grease containing the IF- WS_2 , the base grease was heated up to 60 °C and mixed carefully with 5 wt.% of the IF nanoparticles for 5 h. The effect of the IF-additive to grease was studied using a ring-block tribotester. The lithium grease containing the IF-additive showed better tribological properties than those of grease with 2H- MoS_2 particles. Preservation of the IF nanoparticles on the mating surfaces under friction at a high load provided improved tribological properties of greases with the IF-additives.

Wozniak et al. [61] studied lithium grease with the TiO_2 and ZrO_2 nanoparticles lubricating the mating surfaces in tie rod ends. The steel ball–polymer insert contact zone was lubricated with the pure lithium grease or containing 1 wt.% of TiO_2 or ZrO_2 nanoparticles. Studies on friction were carried out using the tribotester, allowing reversal motion at different contact loads.

The authors of the paper [119] studied the spinning friction in contact zone between steel ball and plate lubricated by lithium grease without and with addition of SiO_2 NPs at constant speed and stepwise increasing contact load. The COF value decreased with an increase of contact load for simple lithium grease. Addition of 6 wt.% of SiO_2 NPs to the grease was conducive to the same trend. However, addition of other concentrations of SiO_2 NPs was conducive to decrease of COF value with an increase of the contact load.

2.4.4. Methods of Preparation of ZrO_2 Nanoparticles

There are three thermodynamically stable crystalline phases of ZrO_2 under atmospheric pressure: monoclinic, tetragonal, and cubic [120–124]. Among all these crystalline phases, the cubic phase has good thermal, mechanical, and electrical properties [125,126].

The stability of zirconia nanoparticles can be increased by addition of trivalent ions (e.g., yttrium ions or aluminum ones) [127,128]. These oxides are commonly called “YSZ” (Yttria Stabilized Zirconia).

According to Reference [129], zirconium oxide (ZrO_2) can be prepared by various techniques such as the sol–gel method, co-precipitation, or hydrothermal processes.

According to Reference [50], there are numerous technologies based on wet chemical methods for synthesis of ZrO_2 nanopowders, such as precipitation methods, mechano-chemical methods, emulsion methods, hydrothermal ones, and others.

Nano-sized yttria doped zirconia can be synthesized by co-precipitation [55] or hydrothermal route [114,127,129–131].

The hydrothermal route allows a good stabilization of YSZ due to its ability to create crystalline phases at low temperature [132].

Rosa et al. [133] synthesized YSZ nanoparticles by the Continuous Hydrothermal Synthesis.

Nanorods from YSZ can be grown by metal–organic chemical vapor deposition (MOCVD) method [134] or using hydrothermal route [135].

The use of sol–gel technology allowed improvement in material processing. Such a process covers organic, inorganic hybrid, and metallic materials [136].

According to Reference [137], the sol–gel technique allowed obtaining nanostructured coatings with enhanced functional or mechanical properties as well as high purity, homogeneity, and improved microstructure.

The sol–gel method does not require vacuum and allows fabricating a large area with low cost and at low processing temperature [138,139].

Bashir et al. [140] synthesized ZnO-doped ZrO₂ nanoparticles using the sol–gel method with different concentrations of ZnO in acidic and basic medium. Zirconyl chloride octahydrate (ZrOCl₂·8H₂O) Ethanol and Deionized (DI) water were used as precursors, whereas NaOH was used as a gelation agent. All materials were of chemical grade and used without further purification. Zirconyl chloride octahydrate (ZrOCl₂·8H₂O) was added to DI water to form solution of molarity 0.1 M and pH = 2. Solution was stirred and heated at 50 °C for 1 h before and after addition of ethanol. Then ZnO was added dropwise from 1 to 5 wt.% into the synthesized sol. All sols were subjected to gel formation by heating at 60 °C to form powder of ZrO₂ nanoparticles.

Ashkarran et al. [141] synthesized ZrO₂ nanoparticles by high current electrical arc discharge of zirconium electrodes in deionized (DI) water. A mixture of nanocrystalline ZrO₂ monoclinic and tetragonal phase was formed. The size of the particles increased with increase of the arc current.

The sol–gel method was used in Reference [142] for preparation of Fe₃O₄-doped ZrO₂ nanoparticles (NPs). The ZrO₂ sol was doped with pre-synthesized Fe₃O₄ NPs resulting in a mixture of monoclinic and tetragonal zirconia. An increase in crystallite size was observed with increase of the dopant concentration. The lattice contraction was observed for the Fe₃O₄-doped ZrO₂ samples. This contraction resulted in volumetric change conducive to formation of tetragonal phase. Relatively high density (~6 g/cm³) was observed.

Arantes et al. [143] obtained nanocrystalline ZrO₂ particles by hydrothermal treatment of 0.25 M ZrO(NO₃)₂ and 0.5 M ZrOCl₂ aqueous solutions at different values of the temperature and time in the presence of hydrogen peroxide. Nanocrystalline monoclinic ZrO₂ powders with a narrow distribution of the 3.5 nm-sized crystallites were obtained. As the crystallization depended strongly on the temperature, an amorphous material was synthesized at 100 °C, and crystalline one with monoclinic phase was obtained at 110 °C, independently of the salt used. ZrO₂ colloidal nanoparticles were obtained only by hydrothermal treatment longer than 24 h.

Danilenko et al. [50] prepared ZrO₂ nanopowders by precipitation.

Palanisamy et al. [144] produced ZrO₂ nanoparticles with non-stabilized monoclinic and sodium-stabilized cubic phase from ZrO₂ sand using ball mill-aided precipitation route.

Vasylykiv and Sakka [49] prepared tetragonal 3 mol% Y₂O₃-doped ZrO₂ nanopowder by hydrothermal precipitation from metal chlorides and urea sol followed by a washing–drying treatment and calcination.

According to Colbea et al. [145], the wet impregnation process of ZrO₂ nanoparticles with 10% and 20% Eu oxide followed by thermal annealing in the air at a temperature above 500 °C allowed obtaining the fully-stable tetragonal phase of ZrO₂. The bare ZrO₂ nanoparticles were obtained through the oil in water microemulsion, rapid hydrothermal treatment, and citrate complexation method.

2.4.5. Agglomeration of ZrO₂ Nanoparticles and Methods to Prevent It

Danilenko et al. [50] stated that the agglomeration degree depends on surface properties of nanoparticles, type of dispersant, and other conditions.

Some reports [146–148] pointed that the precipitation methods with microwave drying, pulse magnetic field treatment, and ultrasonication of Zr hydroxide resulted in formation of small size “soft” Zr hydroxide agglomerates. Subsequent processes of calcination under low temperature allowed obtaining ZrO₂ nanoparticles with predetermined particle size of narrow size distribution and “soft” agglomerates.

Danilenko et al. [50] studied the influence of different surfactants (Trilon B, Polyammoniumacrylate and Neonol) and mineralizers (HCl, KOH, CH₃COOH, etc.) on agglomeration degree of ZrO₂

nanopowders. By adding surfactants and mineralizers, different phase composition, particle size, and agglomeration degree of zirconia nanopowders were obtained. Increasing the specific surface area did not always result in a decrease in the particle size. Additions of KOH and KNO₃ led to an increase in particle size and specific surface area simultaneously. It was affected by a decrease in the agglomeration degree of nanoparticles due to changes in the interaction forces between particles influenced by surfactants and mineralizers. Low calcination temperatures (less than 700 °C) led to the formation of the zirconia particles with cylindrical form. The addition of KNO₃ led to the formation of non-agglomerated cylindrical zirconia particles with a diameter near to 12 nm and a length near to 2–3 nm.

According to Palanisamy et al. [144], the ball-milling process allowed disaggregation of the aggregated ZrO₂ nanoparticles obtained by precipitation. The ball-milling process provided fully crystalline monoclinic ZrO₂ nanoparticles of a size of 64 nm and a specific surface area of 126 m²/g. Furthermore, the sodium-stabilized cubic ZrO₂ nanoparticles with a size of 39 nm and the specific surface area of 227 m²/g were obtained through the ball-milling process.

Vasylykiv and Sakka [49] studied the effects of nanopowder washing by water and ethanol with subsequent centrifuging, with possible deagglomeration using microtip ultrasonication on the properties of ZrO₂ nanopowders. The ultrasonic irradiation induced the pressure waves generating the violently collapsing cavities, producing intense stress. Such stress allowed minimization of secondary particle size, deagglomerating the powder, redispersing the ZrO₂ after all the washing–centrifuging cycles, and minimizing mean aggregate size after final calcination. A uniformly aggregated tetragonal ZrO₂ nanopowder without hard agglomerates was prepared.

The stable dispersion and the reduced agglomeration of the nanoparticles can be achieved via ultrasonication, homogenizing, magnetic force agitation, probe sonication, ball milling, and high shear mixing [149]. Achieving proper dispersion of the nanoparticles needs the reduction of the chance for agglomeration strongly affected by the method and the time duration of dispersion.

According to Reference [48], the surface modification of nanoparticles or using the surfactants can enhance dispersion stability of nanoparticles.

Sui et al. [150] explained that the surface modification of nanoparticles allows tailoring of their surface properties to the use of organic modifying agents. The most used representative of the latter is oleic acid. It absorbs around the nanoparticles reducing their surface energy and, as a result, blocks the agglomeration.

The dispersion stability of nanolubricants can be enhanced by adding surfactants also called dispersants. Such a surfactant can be oleic acid, sodium dodecyl sulfate (SDS), TRITON TMX102, benzalkonium chloride, or benzethonium chloride [151].

According to Reference [48], the addition of the surfactants enhances the dispersion stability of nanoparticles and allows reduction of friction and wear.

According to De Monredon et al. [152], the significant agglomeration of nanoparticles can occur during the sol–gel process involving hydrolysis and condensation, which are generally fast and need to be inhibited to avoid precipitation and allow sol or gel formation.

2.5. Lubrication Mechanism of Lithium Nanogrease

According to Reference [66], the formation of boundary lubrication film highly affects the tribological performance of the lithium nanogrease. The lubricant film contains nanoparticles on the mating surfaces. The mechanism takes place in three stages:

Stage-I: rubbing surfaces come in contact through asperities. The gap between asperities is filled by nanogrease, providing a lubricating effect.

Stage-II: CaF₂ nanoparticles are deposited on the rubbing surfaces. The low shear strength of CaF₂ due to its low size decreases the friction coefficient. The micro-point contact has a high surface pressure and high temperature, facilitating a complex tribochemical reaction.

Stage-III: The reaction product together with CaF_2 nanoparticles form complicated wear-resistant film on the rubbing surface resulting in excellent lubrication at the contact zone.

The mechanism of film formation on the rubbed surfaces was verified and reported by several authors [66–69,118]. The boundary lubricating film was composed of deposited NCB and reaction products such as B_2O_3 , CaO , and iron oxide [67].

According to Reference [153], the layered structured material, such as graphene, as additives to lithium grease, can form conformal protective layer on rubbing surfaces.

According to Reference [154], the planar structure and nano-spaced layer facilitate easy shearing between contacts due to weak van der Waals forces between layers.

Petrone [155] carried out the rheological tests of the lithium greases with the MoS_2 additive obtaining the same results for the grease samples with 2 wt.% nanoparticles and for one with 4 wt.% of MoS_2 . The different types of inorganic nanoparticles, with different concentrations in weight, did not affect the rheological behavior of the lubricating grease. He also carried out tribological tests for steel–steel contact zone using the rotational tribometer. He found a decrease of the friction coefficient both in boundary and mixed lubrication regimes achievable through MoS_2 nanosheets dispersion, with average reduction for lithium grease around 35%. The best performance in terms of wear scar diameter (WSD) was provided by the lithium grease with 2 wt.% of MoS_2 .

The anti-wear property of MoS_2 nanosheets as an additive to the lithium grease was clearly visible in both the abovementioned lubrication regimes, leading to an average decrease level of 30% of the scar diameter measured on the worn surface of the steel ball. The lithium grease with 2 wt.% of MoS_2 performed better than that with 4 wt.% formulation.

The micro ball-bearing rolling of spherical IF-nanoparticles reducing contact area also improves tribological properties of nanogreases [118].

2.6. Tribological Evaluation of Nanogrease

Wang et al. [66] studied the tribological properties of lithium grease containing CaF_2 nanocrystallites with a four-ball tribotester. They obtained a reduction in wear scar diameter by 29% and a decrease of friction by 19% in comparison to those for the base lithium grease. The improvement in tribological properties of CaF_2 -added grease was not proportional to the concentration of CaF_2 and was limited.

Zhao et al. [67] studied tribological properties of lithium grease containing nano-calcium borate (NCB) on an Optimol SRV-IV oscillating reciprocating friction and wear (SRV) tester. The excellent wear-resistant and friction-reducing properties corresponded to an optimal concentration of 6 wt.% of NCB in lithium grease. For the worn steel surface lubricated with lithium grease, a wide wear scar with a deep groove was observed. For worn steel surface lubricated by lithium grease with 6 wt.% of NCB, the wear debris on rubbing surfaces created relatively small, smooth, and shallow wear scar.

During studies on lithium grease with addition of Graphene, Graphene Oxide, and Graphite described in [153], it was found a decrease in coefficient of friction by 30%, 40%, and 60% for grease based on graphene oxide, graphite, and graphene, respectively.

A 63% decrease was reported in wear scar diameter during studies on the lithium grease with addition of 1 wt.% of carbon nanotubes using a four-ball tester [105]. Furthermore, a decrease of COF value by 81% and an increase of the resistance to EP properties and load-carrying capacity by 52% was achieved. During friction process, the mating surfaces were covered by the boundary film containing CNTs, Cr, iron oxide, and other compounds.

Studies described in Reference [117] on lithium grease with addition of TiO_2 and CuO showed a decrease of friction by approximately 40% and 60% for TiO_2 and CuO , respectively.

3. Materials and Methods for Tribological Investigation

3.1. Samples Preparation for Tribological Tests

During friction tests, a polished steel ball of 18 mm diameter rotated with constant speed relative to the fixed counterpart. The ball mates with the polyethylene counterpart of 30 mm inner diameter and fixed in the steel ring. The contact zone was loaded with a constant force and lubricated with lithium grease without or with 1 wt.% amount of ZrO_2 nanoparticles of a size 10–20 nm (for details see Reference [61]). The lithium grease was mixed with the ZrO_2 nanoparticles by the High-Speed Planetary Mixer THINKY SR-5000 [156] followed by treatment with GT Sonic VGT-800 Ultrasonic Cleaner for approximately 120 s in order to avoid agglomeration or the structural break of the nanoparticles. To indicate the occurrence of agglomeration of ZrO_2 nanoparticles, the lithium grease with 1 wt.% of ZrO_2 nanoparticles were left at rest for two weeks from preparation to the beginning of tests in a closed container at 20 °C.

3.2. Investigation of Friction Coefficient

The friction in the steel ball/polymer insert contact zone lubricated by the lithium grease without or with ZrO_2 nanoparticles was studied with the use of a tribotester [61]. The tribotester allowed obtaining values of the spinning friction torque in the contact zone between ball and its counterpart. Measurements were performed under constant rotating speed of 36 rpm of the ball and under constant load in the contact zone that was increased stepwise from 7.2 to 27.2 N. The COF values were calculated using measured values of the friction torque, diameter of contact zone, and an average contact pressure in the contact zone between the ball and its counterpart. The average contact pressure and diameter of the contact zone were estimated using the FEM model of such a zone [61]. The values of the contact pressure did not exceed 38 MPa.

4. Results

The obtained graphs of the friction coefficient as a function of load in the contact zone between steel ball and polyamide inner sphere are presented in Figure 3 for 3 different lubrication systems: with pure lithium grease, with fresh lithium grease containing 1 wt.% of ZrO_2 nanoparticles as the additive without agglomerations of ZrO_2 nanoparticles, and with lithium grease with 1 wt.% of ZrO_2 nanoparticles left at rest for two weeks from preparation to the beginning of the tests in a closed container at 20 °C that provoked occurrence of agglomerations of ZrO_2 nanoparticles.

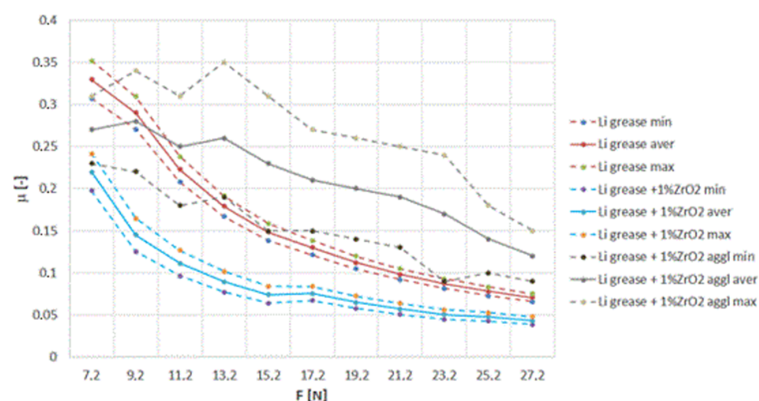


Figure 3. Friction coefficient vs. load in the contact zone between steel ball and polyamide inner sphere for three different lubricating systems: with pure lithium grease, with fresh lithium grease containing 1 wt.% amount of ZrO_2 nanoparticles as the additive without agglomeration, as well as with lithium grease containing 1 wt.% of ZrO_2 nanoparticles left at rest for two weeks from its preparation to the beginning of the tests in a closed container at 20 °C due to which a partial agglomeration of ZrO_2 nanoparticles took place.

For the cases of pure grease and the grease with 1 wt.% of non-agglomerated ZrO₂ nanoparticles, the increase of the load in the contact zone resulted in decrease of the average value of the friction coefficient (COF). The standard deviations of the COF values also decreased with an increase in the load. For grease with 1 wt.% of agglomerated ZrO₂ nanoparticles, the increase of load in the contact zone was conducive to other changes in average values of COF. For smaller values of the load, the average COF value at first decreased and next increased. Further increase of the load resulted in a decrease of the COF value. The standard deviations of the COF values for such a grease were higher than those for pure grease and the grease with non-agglomerated ZrO₂ nanoparticles and varied with increase of the load in the contact zone. For smallest and the highest values, the load and the standard deviations of the COF values were the lowest. For the other values of the load, the standard deviations of the COF values were clearly higher.

5. Discussion and Conclusions

It follows from the survey of lithium grease properties an important effect of additives, particularly of ZrO₂-based nanoparticles on tribological properties of the grease. The agglomeration of such nanoparticles is an unwanted phenomenon, not only during preparation of the lubricant but also during subsequent sintering process of the ZrO₂ nanoparticles. There are several methods of producing ZrO₂ nanoparticles, however, a part of them cannot prevent nanoparticles' agglomeration. For example, the commonly used precipitation method leads to aggregated ZrO₂ nanoparticles, which are next disaggregated by ball-milling. In this context, the method based on ZrO₂ nanopowder washing by water and ethanol with subsequent centrifuging looks interesting, with possible deagglomeration with the use of microtip ultrasonication. The dispersion stability of ZrO₂ nanoparticles in oil or in grease can be enhanced either by surface modification of such nanoparticles or by using the surfactants. The choice of the method of surface modification or of surfactant application is difficult and further investigations are needed for ZrO₂ nanopowders.

There is a clear relationship between tribological properties of lubricants containing nanoparticles and agglomeration of such nanoparticles.

The addition of 1 wt.% ZrO₂ nanoparticles to pure lithium grease decreased COF value by up to 50%, especially for lower values of the load in the contact zone. The occurrence of agglomerations of ZrO₂ nanoparticles in the lithium grease increased COF value twice as compared to that for the pure grease. Moreover, standard deviations of the COF values are significantly higher than those for the lithium grease without agglomerated nanoparticles.

Funding: This research received no external funding.

Conflicts of Interest: The authors declare no conflict of interest.

References

1. Lugt, M. A Review on Grease Lubrication in Rolling Bearings. *Tribol. Trans.* **2009**, *52*, 470–480. [[CrossRef](#)]
2. Barnes, H.A. Thixotropy—A review. *J. Non-Newton. Fluid Mech.* **1997**, *70*, 1–33. [[CrossRef](#)]
3. Paszkowski, M.; Olsztynska-Janus, S. Grease thixotropy: Evaluation of grease microstructure change due to shear and relaxation. *Ind. Lubr. Tribol.* **2014**, *66*, 223–237. [[CrossRef](#)]
4. Paszkowski, M. Identification of the thixotropy of lithium greases. In Proceedings of the 16th International Colloquium Tribology 2008—Lubricants, Materials and Lubrication Engineering, Stuttgart/Ostfildern, Germany, 15–17 January 2008. Volume: Book of Sunopses.
5. Cann, M.; Doner, J.P.; Webster, M.N.; Wikstrom, V. Grease Degradation in Rolling Element Bearings. *Tribol. Trans.* **2001**, *44*, 399–404. [[CrossRef](#)]
6. Lugt, M. *Grease Lubrication in Rolling Bearings*; John Wiley & Sons: Hoboken, NJ, USA, 2012.
7. Cann, M.; Webster, M.N.; Doner, J.P.; Wikstrom, V.; Lugt, P. Grease Degradation in R0F Bearing Tests. *Tribol. Trans.* **2007**, *50*, 187–197. [[CrossRef](#)]

8. Rezasoltani, A.; Khonsari, M. On Monitoring Physical and Chemical Degradation and Life Estimation Models for Lubricating Greases. *Lubricants* **2016**, *4*, 34. [[CrossRef](#)]
9. Huang, L.; Guo, D.; Cann, M.; Wan, G.T.Y.; Wen, S. Thermal Oxidation Mechanism of Polyalphaolefin Greases with Lithium Soap and Diurea Thickeners: Effects of the Thickener. *Tribol. Trans.* **2016**, *59*, 801–809. [[CrossRef](#)]
10. Rezasoltani, A.; Khonsari, M. Experimental investigation of the chemical degradation of lubricating grease from an energy point of view. *Tribol. Int.* **2019**, *137*, 289–302. [[CrossRef](#)]
11. Gurt, A.; Khonsari, M. The Use of Entropy in Modeling the Mechanical Degradation of Grease. *Lubricants* **2019**, *7*, 82. [[CrossRef](#)]
12. Zhou, Y.; Bosman, R.; Lugt, M. On the Shear Stability of Dry and Water-Contaminated Calcium Sulfonate Complex Lubricating Greases. *Tribol. Trans.* **2019**, *62*, 626–634. [[CrossRef](#)]
13. Rezasoltani, A.; Khonsari, M.M. On the Correlation between Mechanical Degradation of Lubricating Grease and Entropy. *Tribol. Lett.* **2014**, *56*, 197–204. [[CrossRef](#)]
14. Rezasoltani, A.; Khonsari, M.M. An engineering model to estimate consistency reduction of lubricating grease subjected to mechanical degradation under shear. *Tribol. Int.* **2016**, *103*, 465–474. [[CrossRef](#)]
15. Hurley, S.; Cann, P.M.; Spikes, H. Lubrication and Reflow Properties of Thermally Aged Greases. *Tribol. Trans.* **2000**, *43*, 221–228. [[CrossRef](#)]
16. Couronne, I.; Vergne, P. Rheological Behavior of Greases: Part II—Effect of Thermal Aging, Correlation with Physico-Chemical Changes. *Tribol. Trans.* **2000**, *43*, 788–794. [[CrossRef](#)]
17. Plint, M.; Alliston-Greiner, A. A New Grease Viscometer: A Study of the Influence of Shear on the Properties of Greases. *NLGI Spokesm.* **1992**, *56*, 7–15.
18. Cyriac, F.; Lugt, M.; Bosman, R. Impact of Water on the Rheology of Lubricating Greases. *Tribol. Trans.* **2016**, *59*, 679–689. [[CrossRef](#)]
19. Karis, T.E.; Kono, R.N.; Jhon, M.S. Harmonic Analysis in Grease Rheology. *J. Appl. Polym. Sci.* **2003**, *90*, 334–343. [[CrossRef](#)]
20. Ide, A.; Asai, Y.; Takayama, A.; Akiyama, M. New Life Prediction Method of the Grease by the Activation Energy. *Tribol. Online* **2011**, *6*, 45–49. [[CrossRef](#)]
21. Zhou, Y.; Bosman, R.; Lugt, M. A Master Curve for the Shear Degradation of Lubricating Greases with a Fibrous Structure. *Tribol. Trans.* **2019**, *62*, 78–87. [[CrossRef](#)]
22. Lundberg, J.; Höglund, E. A New Method for Determining the Mechanical Stability of Lubricating Greases. *Tribol. Int.* **2000**, *33*, 217–223. [[CrossRef](#)]
23. Salomonsson, L.; Stang, G.; Zhmud, B. Oil/Thickener Interactions and Rheology of Lubricating Greases. *Tribol. Trans.* **2007**, *50*, 302–309. [[CrossRef](#)]
24. Liu, J.; Lozano-Perez, S.; Karamched, P.; Holter, J.; Wilkinson, A.J.; Grovenor, C.R.M. Fore-scattered electron imaging of nanoparticles in scanning electron microscopy. *Mater. Sci.* **2019**, *155*, 109814. [[CrossRef](#)]
25. Bondi, A.; Cravath, A.M.; Moore, R.J.; Peterson, W.H. Basic Factors Determining the Structure and Rheology of Lubricating Grease. *Inst. Spokesm.* **1950**, *13*, 12–18.
26. Singera, A.; Barakat, Z.; Mohapatra, S.; Mohapatra, S.S. Chapter 13—Nanoscale Drug-Delivery Systems: In Vitro and In Vivo Characterization. In *Nano-Carriers for Drug Delivery: Nanoscience and Nanotechnology in Drug Delivery*, 1st ed.; Mohapatra, S.S., Ranjan, S., Dasgupta, N., Mishra, R.K., Thomas, S., Eds.; Elsevier: Amsterdam, The Netherlands, 2019; pp. 395–419.
27. Stetefeld, J.; McKenna, S.A.; Patel, T.R. Dynamic light scattering: A practical guide and applications in biomedical sciences. *Biophys. Rev.* **2016**, *8*, 409–427. [[CrossRef](#)]
28. Maguire, C.M.; Rösslein, M.; Wick, P.; Prina-Mello, A. Characterisation of particles in solution—A perspective on light scattering and comparative technologies. *Sci. Technol. Adv. Mater.* **2018**, *19*, 732–745. [[CrossRef](#)]
29. Zimmermann, M.; Ibrom, K.; Jones, G.; Garnweitner, G. Formation of a Dimeric Precursor Intermediate during the Nonaqueous Synthesis of Titanium Dioxide Nanocrystals. *ChemNanoMat* **2016**, *2*, 1073–1076. [[CrossRef](#)]
30. Stolzenburg, P.; Freytag, A.; Bigall, N.C.; Garnweitner, G. Fractal growth of ZrO₂ nanoparticles induced by synthesis conditions. *CrystEngComm* **2016**, *18*, 8396–8405. [[CrossRef](#)]
31. Ninjbadgar, T.; Garnweitner, G.; Börger, A.; Goldenberg, L.M.; Sakhno, O.V.; Stumpe, J. Synthesis of Luminescent ZrO₂:Eu³⁺ Nanoparticles and Their Holographic Sub-Micrometer Patterning in Polymer Composites. *Adv. Funct. Mater.* **2009**, *19*, 1819–1825. [[CrossRef](#)]

32. Bilecka, I.; Niederberger, M. New developments in the nonaqueous and/or non-hydrolytic sol–gel synthesis of inorganic nanoparticles. *Electrochim. Acta* **2010**, *55*, 7717–7725. [[CrossRef](#)]
33. Elbasuney, S. Sustainable steric stabilization of colloidal titania nanoparticles. *Appl. Surf. Sci.* **2017**, *409*, 438–447. [[CrossRef](#)]
34. Aysan, A.B.; Knejzlík, Z.; Ulbrich, P.; Šoltys, M.; Zadražil, A.; Štěpánek, F. Effect of surface functionalisation on the interaction of iron oxide nanoparticles with polymerase chain reaction. *Colloids Surf. B* **2017**, *153*, 69–76. [[CrossRef](#)] [[PubMed](#)]
35. Rashid, Z.; Soleimani, M.; Ghahremanzadeh, R.; Vossoughi, M.; Esmaeili, E. Effective surface modification of MnFe₂O₄@SiO₂@PMIDA magnetic nanoparticles for rapid and high-density antibody immobilization. *Appl. Surf. Sci.* **2017**, *426*, 1023–1029. [[CrossRef](#)]
36. Kockmann, A.; Hesselbach, J.; Zellmer, S.; Kwade, A.; Garnweitner, G. Facile surface tailoring of metal oxide nanoparticles via a two-step modification approach. *RSC Adv.* **2015**, *5*, 60993–60999. [[CrossRef](#)]
37. Cheema, T.; Lichtner, A.; Weichert, C.; Böhl, M.; Garnweitner, G. Fabrication of transparent polymer-matrix nanocomposites with enhanced mechanical properties from chemically modified ZrO₂ nanoparticles. *J. Mater. Sci.* **2012**, *47*, 2665–2674. [[CrossRef](#)]
38. Smoluchowski, M. Mathematical theory of the kinetics of the coagulation of colloidal solutions. *Z. Phys. Chem.* **1917**, *19*, 129–135.
39. Mersmann, A. *Crystallization Technology Handbook*; Taylor & Francis: Abingdon, UK, 2001.
40. Zhang, W.; Crittenden, J.; Li, K.; Chen, Y. Attachment Efficiency of Nanoparticle Aggregation in Aqueous Dispersions: Modeling and Experimental Validation. *Environ. Sci. Technol.* **2012**, *46*, 7054–7062. [[CrossRef](#)]
41. Axford, S.D.T. Aggregation of colloidal silica: Reaction-limited kernel, stability ratio and distribution moments. *J. Chem. Soc. Faraday Trans.* **1997**, *93*, 303–311. [[CrossRef](#)]
42. Hotze, E.M.; Phenrat, T.; Lowry, G.V. Nanoparticle aggregation: Challenges to understanding transport and reactivity in the environment. *J. Environ. Qual.* **2010**, *39*, 1909–1924. [[CrossRef](#)]
43. Stolzenburg, P.; Hämisch, B.; Richter, S.; Huber, K.; Garnweitner, G. Secondary Particle Formation during the Nonaqueous Synthesis of Metal Oxide Nanocrystals. *Langmuir* **2018**, *34*, 12834–12844. [[CrossRef](#)]
44. Rizzuti, A.; Leonelli, C.; Corradi, A.; Caponetti, E.; Martino, D.C.; Nasillo, G.; Saladino, M.L. Structural Characterization of Zirconia Nanoparticles Prepared by Microwave-Hydrothermal Synthesis. *J. Dispers. Sci. Technol.* **2009**, *30*, 1511–1516. [[CrossRef](#)]
45. Rodriguez-Devecchis, V.M.; Carbognani Ortega, L.; Scott, C.E.; Pereira-Almao, P. Use of Nanoparticle Tracking Analysis for Particle Size Determination of Dispersed Catalyst in Bitumen and Heavy Oil Fractions. *Ind. Eng. Chem. Res.* **2015**, *54*, 9877–9886. [[CrossRef](#)]
46. Jazaa, Y.; Lan, T.; Padalkar, S.; Sundararajan, S. The Effect of Agglomeration Reduction on the Tribological Behavior of WS₂ and MoS₂ Nanoparticle Additives in the Boundary Lubrication Regime. *Lubricants* **2018**, *6*, 106. [[CrossRef](#)]
47. Sonali, J.; Sandhyarani, N.; Sajith, V. Tribological properties and stabilization study of surfactant modified MoS₂ nanoparticle in 15W40 engine oil. *Int. J. Fluid Mech. Mach.* **2014**, *1*, 1–5.
48. Srivivas, D.; Charoo, M.S. A Review on Tribological Characterization of Lubricants with Nano Additives for Automotive Applications. *Tribol. Ind.* **2018**, *40*, 594–623. [[CrossRef](#)]
49. Vasykiv, O.; Sakka, Y. Synthesis and Colloidal Processing of Zirconia Nanopowder. *J. Am. Ceram. Soc.* **2001**, *84*, 2489–2494. [[CrossRef](#)]
50. Danilenko, I.; Konstantinova, T.; Pilipenko, N.; Volkova, G.; Glasunova, V. Estimation of Agglomeration Degree and Nanoparticles Shape of Zirconia Nanopowders. *Part. Part. Syst. Charact.* **2011**, *28*, 13–18. [[CrossRef](#)]
51. French, R.A.; Jacobson, A.R.; Kim, B.; Isley, S.L.; Penn, R.L.; Baveye, C. Influence of ionic strength, pH, and cation valence on aggregation kinetics of titanium dioxide nanoparticles. *Environ. Sci. Technol.* **2009**, *43*, 1354–1359. [[CrossRef](#)]
52. Soloviev, A.; Jensen, H.; Søgaard, E.G.; Kanaev, A.V. Aggregation kinetics of sol-gel process based on titanium tetraisopropoxide. *J. Mater. Sci.* **2003**, *38*, 3315–3318. [[CrossRef](#)]
53. Shih, Y.-H.; Liu, W.-S.; Su, Y.-F. Aggregation of stabilized TiO₂ nanoparticle suspensions in the presence of inorganic ions. *Environ. Toxicol. Chem.* **2012**, *31*, 1693–1698. [[CrossRef](#)]
54. Padovini, D.S.S.; Pontes, D.S.L.; Dalmaschio, C.J.; Pontes, F.M.; Longo, E. Facile synthesis and characterization of ZrO₂ nanoparticles prepared by the AOP/hydrothermal route. *RSC Adv.* **2014**, *4*, 38484–38490. [[CrossRef](#)]

55. Nafsin, N.; Hasan, M.; Dey, S.; Castro, R. Effect of ammonia on the agglomeration of zirconia nanoparticles during synthesis and sintering by Spark Plasma Sintering. *Mater. Lett.* **2016**, *183*, 143–146. [CrossRef]
56. Azman, N.F.; Syahrullail, S.; Rahim, E.A. Preparation and dispersion stability of graphite nanoparticles in palm oil. *J. Tribol.* **2018**, *19*, 132–141.
57. Moshkovith, A.; Perfiliev, V.; Verdyan, A.; Lapsker, I.; Popovitz-Biro, R.; Tenne, R.; Rapoport, L. Sedimentation of IF-WS₂ aggregates and a reproducibility of the tribological data. *Tribol. Int.* **2007**, *40*, 117–124. [CrossRef]
58. Xie, H.; Jiang, B.; He, J.; Xia, X.; Pan, F. Lubrication performance of MoS₂ and SiO₂ nanoparticles as lubricant additives in magnesium alloy-steel contacts. *Tribol. Int.* **2016**, *93*, 63–70. [CrossRef]
59. Gulzar, M.; Masjuki, H.H.; Varman, M.; Kalam, M.A.; Mufti, R.A.; Zulkifli, N.W.M.; Yunus, R.; Zahid, R. Improving the AW/EP ability of chemically modified palm oil by adding CuO and MoS₂ nanoparticles. *Tribol. Int.* **2015**, *88*, 271–279. [CrossRef]
60. Kocjan, A.; Logar, M.; Shen, Z. The agglomeration, coalescence and sliding of nanoparticles, leading to the rapid sintering of zirconia nanoceramics. *Sci. Rep.* **2017**, *7*, 2541. [CrossRef]
61. Wozniak, M.; Siczek, K.; Kubiak, P.; Jozwiak, P.; Siczek, K. Researches on Tie Rod Ends Lubricated by Grease with TiO₂ and ZrO₂ Nanoparticles. *J. Phys. Conf. Ser.* **2018**, *1033*, 012006. [CrossRef]
62. Thibault, R.; (Contributing Editor). Grease Basics. *Efficient Plant*. July/August 2009. Available online: <https://www.efficientplantmag.com/2009/07/grease-basics/> (accessed on 26 February 2020).
63. Thibault, R.; (Contributing Editor). Grease Basics Part II: Selection & Applications. *Efficient Plant*. September/October 2009. Available online: <https://www.efficientplantmag.com/2009/09/grease-basics-part-ii-selection-a-applications/> (accessed on 26 February 2020).
64. Mota, V.; Ferreira, L.A. Influence of grease composition on rolling contact wear: Experimental study. *Tribol. Int.* **2009**, *42*, 569–574. [CrossRef]
65. Classification and Characteristics of Grease. KYODO YUSHI Basic Knowledge about Grease. Available online: <https://www.kyodoyushi.co.jp/english/knowledge/grease/category/> (accessed on 21 December 2019).
66. Wang, L.; Wang, B.; Wang, X.; Liu, W. Tribological investigation of CaF₂ nanocrystals as grease additives. *Tribol. Int.* **2007**, *40*, 1179–1185. [CrossRef]
67. Zhao, W.L.G.; Zhao, Q.; Li, W.; Wang, X. Tribological properties of nano-calcium borate as lithium grease additive. *Lubr. Sci.* **2009**, *26*, 43–53. [CrossRef]
68. Wang, L.; Zhang, M.; Wang, X.; Liu, W. The preparation of CeF₃ nanocluster capped with oleic acid by extraction method and application to lithium grease. *Mater. Res. Bull.* **2008**, *43*, 2220–2227. [CrossRef]
69. Ji, X.; Chen, Y.; Zhao, G. Tribological Properties of CaCO₃ Nanoparticles as an Additive in Lithium Grease. *Tribol. Lett.* **2011**, *41*, 113–119. [CrossRef]
70. Prakash, E.; Rajaraman, R.R.; Sivakumar, K. Tribological Studies on Nano-CaCO₃ Additive Mixed Lubricant. *IOSR J. Mech. Civ. Eng.* **2014**, *6*, 68–74.
71. Liu, D.; Zhang, M.; Zhao, G.; Wang, X. Tribological Behavior of Amorphous and Crystalline Overbased Calcium Sulfonate as Additives in Lithium Complex Grease. *Tribol. Lett.* **2011**, *45*, 265–273. [CrossRef]
72. Mohamed, A.; Khattab, A.; Osman, T.A.; Zaki, M. Influence of Nano Grease Composite on Rheological Behaviour. *Int. J. Eng. Res. Appl.* **2013**, *3*, 1126–1131.
73. Kumar, A. Is Lithium Grease the Best Multi-purpose Grease? *Mach. Lubr.* **2014**, *2*, 9.
74. Canter, N. Feature article: Grease additives: Important contributors not to be overlooked. *Tribol. Lubr. Technol.* **2012**, *68*, 28–32, 34–38.
75. Daniel, R.; Paulus, T. *Chapter 11—Introduction to Gate Drives. Lock Gates and Other Closures in Hydraulic Projects*; Butterworth-Heinemann: Oxford, UK, 2019; pp. 705–784.
76. Mang, T.; Dresel, W. *Lubricants and Lubrication*, 2nd ed.; Wiley-VCH Verlag GmbH & Co. KGaA: Weinheim, Germany, 2007; p. 88.
77. Stepina, V.; Vesely, V. *Lubricants and Special Fluids*; Elsevier: Amsterdam, The Netherlands, 1992; p. 703.
78. Andrew, D.L.; Moore, G.G. Lubricating Grease Containing Alkoxylated Amine Corrosion Inhibitor. EP0903398A2, 24 March 1999.
79. King Industries, Inc. *Lubricant Additives Division: Specialty Additives and Synthetic Base Oils for Industrial & Automotive Lubricants, Greases, Metalworking Fluids and Rust Preventives*; King Industries, Inc.: Norwalk, CT, USA, 2012.
80. Singh, T. Tribochemistry EP Activity Assessment of MoS Complexes in Lithium Base Greases. *Adv. Tribol.* **2008**, *2008*, 947543. [CrossRef]

81. Samy, A.; Ali, W.Y. The effect of tin as solid lubricant dispersing lithium grease in reducing friction coefficient and wear in dusty environments. *Metall* **2013**, *67*, 34–39.
82. Thirumalaikumar, A. The Tribological Behaviour of Nanoparticles Mixed Lubricating Oil—Review. *Int. Res. J. Eng. Technol. IRJET* **2017**, *04*, 3217–3228.
83. Battez, A.H.; González Rodríguez, R.; Viesca, J.; Fernández, J.E.; Fernandez, J.; Machado, A.; Chou, R.; Riba, J.A. CuO, ZrO₂ and ZnO Nanoparticles as Antiwear Additive in Oil Lubricants. *Wear* **2008**, *265*, 422–428. [[CrossRef](#)]
84. Battez, A.H.; González, R.; Felgueroso, D.; Fernández, J.E.; del Rocío Fernández, M.; García, M.A.; Peñuelas, I. Wear prevention behaviour of nanoparticle suspension under extreme pressure conditions. *Wear* **2007**, *263*, 1568–1574. [[CrossRef](#)]
85. Radice, S.; Mischler, S. Lubrication properties of Al₂O₃ nanoparticles in aqueous suspensions. *Tribol. Interface Eng. Ser.* **2005**, *48*, 101–105.
86. Casado, J.E.; González, A.F.; Huerga, Á.J.D.R.; Rodríguez-Solla, H.; Díaz-García, M.E. Badía-Laiño, R. Unctuous ZrO₂ nanoparticles with improved functional attributes as lubricant additives. *IOP Publ. Nanotechnol.* **2017**, *28*, 495704. [[CrossRef](#)] [[PubMed](#)]
87. Kumar, M.; Afzal, A.; Ramis, M.K. Investigation of physicochemical and tribological properties of TiO₂ nano-lubricant oil of different concentrations. *Tribol. Finn. J. Tribol.* **2017**, *35*, 6–15.
88. Yu, R.; Liu, J.; Zhou, Y. Experimental Study on Tribological Property of MoS₂ Nanoparticle in Castor Oil. *J. Tribol.* **2019**, *141*, 102001. [[CrossRef](#)]
89. Jendrzrej, S.; Gökce, B.; Barcikowski, S. Colloidal Stability of Metal Nanoparticles in Engine Oil under Thermal and Mechanical Load. *Chem. Eng. Technol.* **2017**, *40*, 1569–1576. [[CrossRef](#)]
90. Hwang, J.; Lee, C.; Choi, Y.; Cheong, S.; Kim, D.; Lee, K.; Lee, J.; Kim, S.H. Effect of the size and morphology of particles dispersed in nano-oil on friction performance between rotating discs. *J. Mech. Sci. Technol.* **2011**, *25*, 2853–2857. [[CrossRef](#)]
91. Joly-Pottuz, L.; Dassenoy, F.; Belin, M.; Vacher, B.; Martin, J.M.; Fleisher, N. Ultralow-friction and wear properties of IF-WS₂ under boundary lubrication. *Tribol. Lett.* **2005**, *18*, 477–485. [[CrossRef](#)]
92. Cizaire, L.; Vacher, B.; Le Mogne, T.; Martin, J.M.; Rapoport, L.; Margolin, A.; Tenne, R. Mechanisms of ultra-low friction by hollow inorganic fullerene-like MoS₂ nanoparticles. *Surf. Coat. Technol.* **2002**, *160*, 282–287. [[CrossRef](#)]
93. Joly-Pottuz, L.; Dassenoy, F. *Nanolubricants*; John Wiley & Sons, Ltd.: Hoboken, NJ, USA, 2008; pp. 15–92.
94. Hu, K.; Hu, X.; Xu, Y.; Huang, F.; Liu, J. The effect of morphology on the tribological properties of MoS₂ in liquid paraffin. *Tribol. Lett.* **2010**, *40*, 155–165. [[CrossRef](#)]
95. Rapoport, L.; Moshkovich, A.; Perfilyev, V.; Laikhtman, A.; Lapsker, I.; Yadgarov, L.; Rosentsveig, R.; Tenne, R. High lubricity of Re-doped fullerene-like MoS₂ nanoparticles. *Tribol. Lett.* **2012**, *45*, 257–264. [[CrossRef](#)]
96. Yadgarov, L.; Petrone, V.; Rosentsveig, R.; Feldman, Y.; Tenne, R.; Senatore, A. Tribological studies of rhenium doped fullerene-like MoS₂ nanoparticles in boundary, mixed and elasto-hydrodynamic lubrication conditions. *Wear* **2013**, *297*, 1103–1110. [[CrossRef](#)]
97. Aralihalli, S.; Biswas, S. Grafting of dispersants on MoS₂ nanoparticles in base oil lubrication of steel. *Tribol. Lett.* **2013**, *49*, 61–76. [[CrossRef](#)]
98. Anand, G.; Saxena, P. A review on graphite and hybrid nano-materials as lubricant additives. *IOP Conf. Ser. Mater. Sci. Eng.* **2016**, *149*, 012201. [[CrossRef](#)]
99. Zhornik, V.I.; Ivakhnik, A.V.; Ivakhnik, V.P. Nanocalcite-Based Greases. *Nanosci. Technol. Int. J.* **2013**, *4*, 281–288. [[CrossRef](#)]
100. Mohamed, A.; Ali, S.; Osman, T.A.; Kamel, B.M. Development and manufacturing an automated lubrication machine test for nano grease. *J. Mater. Res. Technol.* **2019**. [[CrossRef](#)]
101. Mobasher, A.; Khalil, A.; Khashaba, M.; Osman, T. Effect of MWCNTs/Talc powder nanoparticles on the tribological and thermal conductivity performance of calcium grease. *Ind. Lubr. Tribol.* **2019**, *72*, 9–14. [[CrossRef](#)]
102. Younes, H.; Christensen, G.; Groven, L.; Hong, H.; Smith, P. Three dimensional (3D) percolation network structure: Key to form stable carbon nano grease. *J. Appl. Res. Technol.* **2016**, *14*, 375–382. [[CrossRef](#)]
103. Hu, E.Z.; Xu, Y.; Hu, K.H.; Hu, X.G. Tribological properties of 3 types of MoS₂ additives in different base greases. *Lubr. Sci.* **2017**, *29*, 541–555. [[CrossRef](#)]

104. He, Q.; Li, A.; Guo, Y.; Liu, S.; Kong, L.-H. Effect of nanometer silicon dioxide on the frictional behavior of lubricating grease. *Nanomater. Nanotechnol.* **2017**, *7*, 1–9. [CrossRef]
105. Mohamed, A.; Osman, T.A.; Khattab, A.; Zaki, M. Tribological Behavior of Carbon Nanotubes as an Additive on Lithium Grease. *ASME J. Tribol.* **2015**, *137*, 011801. [CrossRef]
106. Xia, X.T.; Zhang, Y.P.; Zhang, Y.Z.; Chen, S.C. Influence of ZrO₂ Nanoparticle as Additive on Tribological Property of Lithium Grease. *Appl. Mech. Mater.* **2010**, 26–28, 83–87. [CrossRef]
107. Li, T.; Pan, B.; Wang, C.; Zhang, S.; Huang, S. Effect of eco-friendly carbon microspheres on the tribological behavior of lithium lubricating grease. *UPB Sci. Bull. Ser. B* **2019**, *81*, 57–68.
108. Ashour, M.E.; Osman, T.A.; Khattab, A.; Elshalakny, A.B. Novel Tribological Behavior of Hybrid MWCNTs/MLNGPs as an Additive on Lithium Grease. *J. Tribol.* **2017**, *139*, 041801. [CrossRef]
109. Wang, J.; Guo, X.; He, Y.; Jiang, M.; Zhou, W. Synthesis and tribological properties of graphene-copper nanoparticles composites. *China Pet. Process. Petrochem. Technol.* **2017**, *19*, 113–122.
110. Wang, J.; Guo, X.; He, Y.; Jiang, M.; Guo, W.; Zhang, Y.; Sun, R. Tribological characteristics of graphene as lithium grease additive. *China Pet. Process. Petrochem. Technol.* **2017**, *19*, 46–54.
111. Zheng, B.; Zhou, J.; Jia, X.; He, Q. Friction and wear property of lithium grease contained with copper oxide nanoparticles. *Appl. Nanosci.* **2019**. [CrossRef]
112. NanoLub® GH-X Lithium EP Grease Additive. NanoMaterials, Ltd. An NIS Corporation. Available online: <http://www.apnano.com/products/nanolub-gh-x-lithium-ep-grease-additive/> (accessed on 21 December 2019).
113. Zhang, Z.; Liu, W.; Xue, Q. Friction and wear behaviors of the complexes of rare earth hexadecylate as grease additive. *Wear* **1998**, *215*, 40–45. [CrossRef]
114. Piticescu, R.; Monty, C.; Taloi, D.; Motoc, A.; Axinte, S. Hydrothermal synthesis of zirconia nanomaterials. *J. Eur. Ceram. Soc.* **2001**, *21*, 2057–2060. [CrossRef]
115. Zhang, X.; Zhang, Z.; Zhao, F.; Qiu, T. Preparation and tribological properties of Bi nanoparticles as a lithium grease additive. *Optoelectron. Adv. Mater. Rapid Commun.* **2014**, *8*, 500–505.
116. Lu, A.; Niu, W.; Dai, Y.; Xu, H.; Dong, J. Tribological Properties of ZnS(NH₂CH₂CH₂NH₂)_{0.5} and ZnS as Additives in Lithium Grease. *Lubricants* **2019**, *7*, 26. [CrossRef]
117. Chang, H.; Lan, C.W.; Chen, C.H.; Kao, M.J.; Guo, J.B. Anti-wear and friction properties of nanoparticles as additives in the lithium grease. *Int. J. Precis. Eng. Manuf.* **2014**, *15*, 2059–2063. [CrossRef]
118. Rapoport, L.; Leshchinky, V.; Volovik, Y.; Lvovsky, M.; Nepomnyashchy, O.; Feldman, Y.; Popovitz-Biro, R.; Tenne, R. Modification of contact surfaces by fullerene-like solid lubricant nanoparticles. *Surf. Coat. Technol.* **2003**, 163–164, 405–412. [CrossRef]
119. Rylski, A.; Siczek, K. Investigation of tribological properties of lithium grease with SiO₂ nanoparticles. *IOP Conf. Ser. Mater. Sci. Eng.* **2019**, *551*, 012012. [CrossRef]
120. Srinivasan, R.; De Angelis, R.J.; Ice, G.; Davis, B.H. Identification of tetragonal and cubic structures of zirconia using synchrotron x-radiation source. *J. Mater. Res.* **1991**, *6*, 1287–1292. [CrossRef]
121. Bokhimi, X.; Morales, A.; Novaro, O.; Portilla, M.; Lopez, T.; Tzompantzi, F.; Gomez, R. Tetragonal nanophase stabilization in nondoped sol–gel zirconia prepared with different hydrolysis catalysts. *J. Solid State Chem.* **1998**, *135*, 28–35. [CrossRef]
122. Sayilkan, F.; Asiltürk, M.; Burunkaya, E.; Arpaç, E. Hydrothermal synthesis and characterization of nanocrystalline ZrO₂ and surface modification with 2-acetoacetoxyethyl methacrylate. *J. Sol-Gel Sci. Technol.* **2009**, *51*, 182–189.
123. Rauwel, E.; Dubourdieu, C.; Holländer, B.; Rochat, N.; Ducroquet, F.; Rossell, M.; Van Tendeloo, G.; Pelissier, B. Stabilization of the cubic phase of HfO₂ by Y addition in films grown by metal organic chemical vapor deposition. *Appl. Phys. Lett.* **2006**, *89*, 012902. [CrossRef]
124. Nakamura, T.; Sakamoto, Y.; Saji, K.; Sakata, J. NO_x decomposition mechanism on the electrodes of a zirconia-based amperometric NO_x sensor. *Sens. Actuators B Chem.* **2003**, *93*, 214–220. [CrossRef]
125. Joo, J.; Yu, T.; Kim, Y.W.; Park, H.M.; Wu, F.; Zhang, J.Z.; Hyeon, T. Multigram scale synthesis and characterization of monodisperse tetragonal zirconia nanocrystals. *J. Am. Chem. Soc.* **2003**, *125*, 6553–6557. [CrossRef] [PubMed]
126. Herrera, A.M.; de Oliveira, A.A.A.M.; de Oliveira, N.; Hotza, D. Processing and characterization of yttria-stabilized zirconia foams for high-temperature applications. *J. Ceram.* **2013**, *2013*, 785210. [CrossRef]

127. Kholam, Y.; Deshpande, A.; Patil, A.; Potdar, H.; Deshpande, S.; Date, S. Synthesis of yttria stabilized cubic zirconia (YSZ) powders by microwave-hydrothermal route. *Mater. Chem. Phys.* **2001**, *71*, 235–241. [[CrossRef](#)]
128. Brossmann, U.; Albu, M.; Hofer, F.; Würschum, R. Single grain analysis on a nanoscale in ZrO₂: Al₂O₃ nano-composites by means of high-resolution scanning transmission electron microscopy. *Mater. Res. Exp.* **2016**, *3*, 125009. [[CrossRef](#)]
129. Tsukada, T.; Venigalla, S.; Morrone, A.A.; Adair, J.H. Low-Temperature Hydrothermal Synthesis of Yttrium-Doped Zirconia Powders. *J. Am. Ceram. Soc.* **1999**, *82*, 1169–1174. [[CrossRef](#)]
130. Dell’Agli, G.; Mascolo, G. Hydrothermal synthesis of ZrO₂-Y₂O₃ solid solutions at low temperature. *J. Eur. Ceram. Soc.* **2000**, *20*, 139–145. [[CrossRef](#)]
131. Sato, K.; Horiguchi, K.; Nishikawa, T.; Yagishita, S.; Kuruma, K.; Murakami, T.; Abe, H. Hydrothermal Synthesis of Yttria-Stabilized Zirconia Nanocrystals with Controlled Yttria Content. *Inorg. Chem.* **2015**, *54*, 7976–7984. [[CrossRef](#)]
132. Komarneni, S. Nanophase materials by hydrothermal, microwave-hydrothermal and microwave-solvothermal methods. *Curr. Sci.* **2003**, *85*, 1730–1734.
133. Rosa, M.; Gooden, N.; Butterworth, S.; Zielke, P.; Kiebach, R.; Xu, Y.; Gadea, C.; Esposito, V. Zirconia nano-colloids transfer from continuous hydrothermal synthesis to inkjet printing. *J. Eur. Ceram. Soc.* **2019**, *39*, 2–8. [[CrossRef](#)]
134. Chen, C.-C.; Cheng, W.-Y.; Lu, S.-Y.; Lin, Y.-F.; Hsu, Y.-J.; Chang, K.-S.; Kang, C.-H.; Tung, K.-L. Growth of zirconia and yttria-stabilized zirconia nanorod arrays assisted by phase transition. *CrystEngComm* **2010**, *12*, 3664–3669. [[CrossRef](#)]
135. Yadav, K.; Gupta, A.; Sharma, M.; Dabas, N.; Ganguli, A.; Jha, M. Low temperature synthesis process of stabilization of cubic yttria stabilized zirconia spindles: An important high temperature ceramic material. *Mater. Res. Express* **2017**, *4*, 105044. [[CrossRef](#)]
136. Esposito, S.; Turco, M.; Bagnasco, G.; Cammarano, C.; Pernice, P. New insight into the preparation of copper/zirconia catalysts by sol–gel method. *Appl. Catal. A* **2011**, *403*, 128–135. [[CrossRef](#)]
137. Costacurta, S.; Falcaro, P.; Vezzu, S.; Colasuonno, M.; Scopece, P.; Zanchetta, E.; Guglielmi, M.; Patelli, A. Fabrication of functional nanostructured coatings by a combined sol–gel and plasma-enhanced chemical vapour deposition method. *J. Sol-Gel Soc. Technol.* **2011**, *60*, 340–346. [[CrossRef](#)]
138. Riaz, S.; Bashir, M.; Hussain, S.S.; Naseem, S. Effect of Mn-doping concentration on the structural & magnetic properties of sol-gel deposited ZnO diluted magnetic semiconductor. *Int. Conf. Adv. Comput. Sci. Electron. Inf. (ICACSEI 2013)* **2013**, *41*, 316–326.
139. Saeed, M.A.; Riaz, S.; Noor, R.; Naseem, S. Optical and Structural Properties of ZnO Thin Films for Solar Cell Applications. *Adv. Sci. Lett.* **2013**, *19*, 834–838.
140. Bashir, M.; Ashraf, R.; Imtiaz, M.; Riaz, S.; Naseem, S. Synthesis and Characterization of ZrO₂-ZnO Nanoparticles. In Proceedings of the 2013 World Congress on Advances in Nano, Biomechanics, Robotics, and Energy Research, Seoul, Korea, 25–28 August 2013; pp. 316–326.
141. Ashkarran, A.A.; Aghigh, S.M.; Afshar, S.A.A.; Kaviani-pour, M.; Ghoranneviss, M. Synthesis and Characterization of ZrO₂ Nanoparticles by an Arc Discharge Method in Water. *Synth. React. Inorg. Met. Nano Met. Chem.* **2011**, *41*, 425–428.
142. Naseem, S.; Riaz, S.; Bashir, M. Synthesis and Characterization of Fe₃O₄ stabilized ZrO₂ Nanoparticles. In Proceedings of the 2014 World Congress on Advances in Civil, Environmental, and Materials Research (ACEM14), Busan, Korea, 24–28 August 2014.
143. Arantes, T.M.; Mambri, G.P.; Stroppa, D.G.; Leite, E.; Longo, E.; Ramirez, A.; Camargo, E. Stable colloidal suspensions of nanostructured zirconium oxide synthesized by hydrothermal process. *J. Nanopart Res.* **2010**, *12*, 3105–3110. [[CrossRef](#)]
144. Palanisamy, M.; Rajendran, V.; Prema, R.; Bhakta, S.; Bishvanwasha, P. Synthesis of Monoclinic and Cubic ZrO₂ Nanoparticles from Zircon. *J. Am. Ceram. Soc.* **2011**, *94*, 1410–1420.
145. Colbea, C.; Avram, D.; Cojocaru, B.; Negrea, R.; Ghica, C.; Kessler, V.G.; Seisenbaeva, G.A.; Parvulescu, V.; Tiseanu, C. Full Tetragonal Phase Stabilization in ZrO₂ Nanoparticles Using Wet Impregnation: Interplay of Host Structure, Dopant Concentration and Sensitivity of Characterization Technique. *Nanomaterials* **2018**, *8*, 988. [[CrossRef](#)] [[PubMed](#)]

146. Pilipenko, N.P.; Danilenko, I.A.; Konstantinova, T.E.; Dobrikov, A.A.; Dekanenko, V.M.; Volkova, G.K. Influence of ZrO₂-3 mol.% Y₂O₃ powders ultrasonic treatment on physico-mechanical properties of ceramics. *Funct. Mater.* **1998**, *5*, 221–225.
147. Alekseenko, V.I.; Volkova, G.K.; Danilenko, I.A.; Dobrikov, A.A.; Konstantinova, T.E.; Datsko, O.I. Effect of Pulsed Magnetic Field on the Thermal Decomposition of Zirconium Hydroxide. *Inorg. Mater.* **2000**, *36*, 908–911. [[CrossRef](#)]
148. Pilipenko, N.P.; Konstantinova, T.E.; Tokiy, V.V.; Danilenko, I.A.; Saakjants, V.P.; Primisler, V.B. Peculiarities of zirconium hydroxide microwave drying process. *Funct. Mater.* **2002**, *9*, 545–549.
149. Dubey, M.K.; Bijwe, J.; Ramakumar, S.S.V. Effect of dispersant on nano-PTFE based lubricants on tribo-performance in fretting wear mode. *RSC Adv.* **2016**, *6*, 22604–22614. [[CrossRef](#)]
150. Sui, T.; Song, B.; Zhang, F.; Yang, Q. Effects of functional groups on the tribological properties of hairy silica nanoparticles as an additive to polyalphaolefin. *RSC Adv.* **2016**, *6*, 393–402. [[CrossRef](#)]
151. Peng, D.X.; Chen, C.H.; Kang, Y.; Chang, Y.P.; Chang, S.Y. Size effects of SiO₂ nanoparticles as oil additives on tribology of lubricant. *Ind. Lubr. Tribol.* **2010**, *62*, 111–120. [[CrossRef](#)]
152. De Monredon, S.; Cellot, A.; Ribot, F.; Sanchez, C.; Armelao, L.; Gueneau, L.; Delattre, L. Synthesis and characterization of crystalline tin oxide nanoparticles. *J. Mater. Chem.* **2002**, *12*, 2396–2400. [[CrossRef](#)]
153. Cheng, Z.L.; Qin, X.X. Study on friction performance of graphene-based semi-solid grease. *Chin. Chem. Lett.* **2014**, *25*, 1305–1307. [[CrossRef](#)]
154. Tenne, R. Fullerene-like materials and nanotubes from inorganic compounds with a layered (2-D) structure. *Colloids Surf. A. Physicochem. Eng. Asp.* **2002**, *208*, 83–92. [[CrossRef](#)]
155. Petrone, V. Novel Nanoscale Friction Modifiers—Piezoviscosity Effect in EHL Contacts. Advances in Lubrication Technology and Modelling XII Ciclo N.S. (2011–2013). Ph.D. Thesis, Università degli Studi di Salerno, Fisciano, Italy, 2014.
156. Planetary Centrifugal Mixer “THINKY MIXER” AR-100. Available online: <http://www.thinkyusa.com/products/item-all/rotation-revolution-mixer/ar-100.html> (accessed on 21 December 2019).



© 2020 by the authors. Licensee MDPI, Basel, Switzerland. This article is an open access article distributed under the terms and conditions of the Creative Commons Attribution (CC BY) license (<http://creativecommons.org/licenses/by/4.0/>).